Geometrical interpretation of the argument of weak values of general observables in *N*-level quantum systems

Quantum Science and Technology

PAPER

Geometrical interpretation of the argument of weak values of general observables in *N*-level quantum systems

Lorena Ballesteros Ferraz[1,*], **Dominique L Lambert**[2] and **Yves Caudano**[1,*]

[1] Research Unit Lasers and Spectroscopies (UR-LLS), naXys & NISM, University of Namur, Rue de Bruxelles 61, B-5000 Namur, Belgium

[2] ESPHIN & naXys, University of Namur, Rue de Bruxelles 61, B-5000 Namur, Belgium

[*] Authors to whom any correspondence should be addressed.

E-mail: lorena.ballesteros@unamur.be and yves.caudano@unamur.be

Keywords: weak measurement, weak value, geometric phase, generalized Bloch sphere, Bargmann invariant, geodesic triangle, symplectic area

OPEN ACCESS

RECEIVED
23 February 2022

REVISED
2 August 2022

ACCEPTED FOR PUBLICATION
23 August 2022

PUBLISHED
13 September 2022

Abstract

Observations in quantum weak measurements are determined by complex numbers called weak values. We present a geometrical interpretation of the argument of weak values of general Hermitian observables in N-dimensional quantum systems in terms of geometric phases. We formulate an arbitrary weak value in terms of three real vectors on the unit sphere in N^2-1 dimensions, S^{N^2-2}. These vectors are linked to the initial and final states, and to the weakly measured observable, respectively. We express pure states in the complex projective space of $N-1$ dimensions, $\mathbb{C}\mathrm{P}^{N-1}$, which has a non-trivial representation as a $2N-2$ dimensional submanifold of S^{N^2-2} (a generalization of the Bloch sphere for qudits). The argument of the weak value of a projector on a pure state of an N-level quantum system describes a geometric phase associated to the symplectic area of the geodesic triangle spanned by the vectors representing the pre-selected state, the projector and the post-selected state in $\mathbb{C}\mathrm{P}^{N-1}$. We then proceed to show that the argument of the weak value of a general observable is equivalent to the argument of an effective Bargmann invariant. Hence, we extend the geometrical interpretation of projector weak values to weak values of general observables. In particular, we consider the generators of $\mathrm{SU}(N)$ given by the generalized Gell–Mann matrices. Finally, we study in detail the case of the argument of weak values of general observables in two-level systems and we illustrate weak measurements in larger dimensional systems by considering projectors on degenerate subspaces, as well as Hermitian quantum gates. To conclude, we discuss the interpretation and usefulness of geometric phases in weak values in connection to weak measurements.

1. Introduction

Measurement are crucial to quantum technologies [1–6] to extract information from quantum systems [7, 8]. The most common type is the ideal and non-reversible, i.e. projective, measurement that randomly collapses the system state to one eigenstate of the measured observable. Von Neumann developed a model of the interaction between the system and the device that describes their joint evolution during a quantum measurement [9]. The stronger the interaction, the more information the measurement provides but, inevitably as well, the larger the system disturbance [10, 11]. Quantum weak measurements involve minimal interactions between a measuring device, also called the ancilla, and the system: they arise when the ancilla state couples very weakly with the system state [12, 13]. Weakness is defined by the validity of a first-order perturbation expansion of the unitary operator specifying the evolution of the complete quantum state (including both the system itself and the ancilla). When measuring a system observable $\hat{A}$ in the von Neumann scheme, the joint evolution to first order in the coupling strength g is typically given by $\hat{U} \approx \hat{\mathbb{1}} - \mathrm{i}g\hat{A} \otimes \hat{p}$, where $\hat{p}$ represents the ancilla's canonical momentum. This evolution entangles the system and ancilla states, so that the knowledge of the ancilla state at the end of the measurement process

provides information on the system observable. Advantageously, the weak interaction preserves the system initial state $|\psi_i\rangle$ in the limit of small coupling strength. Weak measurements have thus many theoretical and practical applications [8, 13, 14].

In what is frequently called a weak measurement in the literature, the measurement weakness is considered in conjunction with the post-selection of the system state. Post-selection is equivalent to constraining the final state to a particular state $|\psi_f\rangle$. Operationally, it is performed by a strong, projective, final, measurement of the system consecutively to the weak interaction: the measurement of the ancilla is then conditional on successfully obtaining $|\psi_f\rangle$. The projection impacts the ancilla state, shifting its wavefunction centroid by a quantity that is related to what is called the weak value of the observable $\hat{A}$ for the initial and final states [14]:

$$A_w = \frac{\langle\psi_f|\hat{A}|\psi_i\rangle}{\langle\psi_f|\psi_i\rangle} = \frac{\mathrm{Tr}(\hat{\Pi}_f\hat{A}\hat{\Pi}_i)}{\mathrm{Tr}(\hat{\Pi}_f\hat{\Pi}_i)}, \tag{1}$$

where $\hat{\Pi}_i = |\psi_i\rangle\langle\psi_i|$ and $\hat{\Pi}_f = |\psi_f\rangle\langle\psi_f|$ are the projectors on the initial (pre-selected) and final (post-selected) system states, respectively. The conditional ancilla measurement provides information on the observable that is related to both the initial and final states, through the weak value. Weak values are unbounded complex numbers. In typical settings, experimental observations are proportional to the real or to the imaginary part of the weak value [15]. The ancilla wavefunction shift may become very large when the pre- and post-selected states are nearly orthogonal, as can be seen from the denominator of equation (1), a feature exploited extensively in the literature, called 'weak value amplification' [12, 14]. In practice, due to the weak system–ancilla coupling, the experimental determination of the weak value requires an average over many measurements, especially with large amplification, as the post-selection probability is approximately given by the overlap between the initial and final states ($|\langle\psi_f|\psi_i\rangle|^2$).

Metrology [16–18], sensing [19–22] and control of tiny experimental parameters [23, 24] benefit largely from weak value amplification [25, 26]. Weak measurements evidenced new physical phenomena, such as minute optical effects in beam propagation [27–30]. As complex numbers, weak values give a direct access to the complex components of the quantum state in quantum tomography [31–33]. Weak values also provide essential insights into issues related to quantum foundations [34–36], such as paradoxes [37–40] or non-perturbative sensing of quantum particles along trajectories [41–43]. Weak values have also the potential to benefit quantum computing and quantum information processing [44–49].

Although their experimental and practical usefulness is undeniable, there have been many difficulties and recurring debates in interpreting weak values [13, 14, 36]. In view of their significance, we provide a geometric description to clarify their meaning in dispassionate terms. In connection with experimental observations, weak values are usually discussed in terms of their real and imaginary parts [13–15]. Instead, we studied them in the polar representation, in terms of modulus and argument, observable in the meter quantum phase space. This approach leads to a geometrical interpretation of the argument of weak values in terms of geometric phases. When a quantum system evolves, it gives rise to two different types of phases: the dynamical phase, related to the time evolution of the system, and the geometric phase (also called Pancharatnam phase, Berry phase or Pancharatnam–Berry phase), related to the intrinsic geometry of the system state space. It was discovered independently on several occasions [50–53]. In the 50s, Pancharatnam defined the geometric phase as the difference of phase acquired by light along a cyclic polarization trajectory [51], which generalizes to quantum systems following an adiabatic and cyclic evolution, as Berry showed [53]. Later on, it was discovered that neither the adiabatic condition nor the cyclic one were necessary [54–56]. Any quantum system evolving from an initial state to a final one describes a geometrical phase [57]. Sjöqvist recognized the connection existing between weak values and geometric phases [58]. Tamate *et al* studied the geometric phase in quantum erasers and therefrom identified the Pancharatnam phase in weak measurements [59]. Using the Majorana representation (which represents states of N-level system as $N-1$ stars on the Bloch sphere), Cormann and Caudano investigated geometric phases in weak measurements for some specific cases, including Pauli matrices[3] and weak values of projectors on pure states [61]. Ho and Imoto related the polar decomposition of modular values to geometric phases as well [62]. Geometric phases in weak measurements were also considered in the context of the spin Hall effect of light [63, 64] and for sequential measurements [65]. The link between weak values and the Bargmann invariant [66] was noted on multiple occasions [58, 59, 61, 67]. However, there is a lack of a general formalism to study the geometric phase of arbitrary weak values and to understand their geometrical properties in larger dimensions, beyond the special case of the qubit.

[3] Technically, they studied the case of modular values [60], which appear in quantum controlled gates [49], where the weakly measured operator in (1) is unitary rather than Hermitian.

We provide for the first time to our knowledge a geometric description of the weak values of general observables in N-dimensional quantum systems. The space of traceless Hermitian operators acting on an N-dimensional Hilbert space is of dimensions N^2-1. As a result, to any observable, we can associate a real vector on S^{N^2-2}, the unit sphere in N^2-1 dimensions. Since any pure state can be represented by a projector, a Hermitian operator, the pre-selected and post-selected states can also be assigned to points on S^{N^2-2}. Thus, we describe any weak value starting from three real vectors on S^{N^2-2}. When the observable corresponds to a projector on a pure state, all three vectors belong in addition to the complex projective space $\mathbb{C}\mathrm{P}^{N-1}$ [68]. This space has a representation as a non-trivial subspace of S^{N^2-2}, which generalizes the Bloch sphere [69–71]. In the case of two-level systems, i.e. $\mathbb{C}\mathrm{P}^1$, the space of pure states is fully equivalent to the complete surface of the two-sphere S^2: this is the well-known Bloch sphere representation of qubits. When considering three-level and higher level systems, their pure state space, $\mathbb{C}\mathrm{P}^2, \ldots, \mathbb{C}\mathrm{P}^{N-1}$, is not equivalent to the complete surface of a larger unit sphere. All pure states are on the surface of the sphere S^{N^2-2} but all points on the surface do not represent a quantum state. In the state manifold, the three projectors characterizing the pre-selected state, the probed projector observable, and the post-selected state define a geodesic triangle: the vertices are the three states and the edges are the geodesics connecting them (defined using the Fubini–Study metric). The argument of the weak value of a projector $\hat{\Pi}_r$ equals the argument of the Bargmann invariant of the three states $\mathrm{Tr}(\hat{\Pi}_f\hat{\Pi}_r\hat{\Pi}_i)$ (see third member of (1) with $\hat{A}=\hat{\Pi}_r$). This invariant is proportional to the symplectic area[4] of the geodesic triangle [73–75]. The argument of the weak value $\hat{\Pi}_{r,w}$ is thus equal to the Pancharatnam–Berry phase that would be generated by a cyclic evolution of the system quantum state along the edges of the geodesic triangle. When the observable $\hat{A}$ is not a projector, it does not belong to the quantum state manifold and it cannot be the vertex of a geodesic triangle. However, we show that the argument of the weak value of any observable is linked to the argument of an effective Bargmann invariant, defined from a very specific projector. Therefore, the argument of the weak value always corresponds to a geometric phase. We will show how the geometric phase manifests itself in the meter phase space and how the argument of the weak value relates to contextuality, to dynamical and interferometric processes, and to the relative action of $\hat{A}$ as a measured observable or as a generator of unitary transformations.

The following of the paper is organized as follows. After a brief review of the qubit case, we first derive the expression of weak values of projectors on pure states in qutrit systems in terms of vectors on S^7 that also belong to $\mathbb{C}\mathrm{P}^2$ and we find the weak value argument. In a second step, we generalize these results to projectors in N-level systems. We then determine the expression of weak values of general observables with real vectors on S^{N^2-2} and give their argument using an effective Bargmann invariant. Then, we consider the particular case of the generators of $\mathrm{SU}(N)$ given by the generalized Gell–Mann matrices, which are traceless Hermitian observables generalizing the Pauli matrices in N-level systems. Finally, before concluding, we consider a few situations to apply our formalism to: we study the case of a general observable in $\mathrm{SU}(2)$; we discuss projectors on degenerate subspaces and Hermitian quantum gates; and we illustrate the expressions for average values and the quantum uncertainties that result from considering identical pre- and post-selected states. To conclude, we discuss the relevance of the argument of weak values, in particular in the context of weak measurements. A few technical calculations were put in appendices, along with auxiliary contextualization of our work. In particular, in appendices A and B, we explicit our conventions used for $\mathrm{SU}(N)$ generators, projectors, and the star product. We consigned the details of the computation of the weak value to appendix C. Finally, in appendices D and E, we provide additional information about the geometry of states on the generalized Bloch spheres and about the related star and wedge products.

2. Weak values of projectors in $\mathbb{C}^2$ and $\mathbb{C}^3$

We introduce here the basics of the geometric representation on the Bloch sphere of the argument of the weak value of qubit projectors. Then, we relate the argument of the weak value of projectors to Bargmann invariants and geometric phases (in all dimensions). Afterward, we extend the description from two- to three-level systems. Throughout this paper, we will always consider pure pre- and post-selected states.

Most generally, pure quantum states are represented by projectors $\hat{\Pi}_r=|\psi_r\rangle\langle\psi_r|$ in complex projective space (they verify $\hat{\Pi}_r^2=\hat{\Pi}_r$). The state space of two-level quantum systems corresponds to the complex projective line $\mathbb{C}\mathrm{P}^1$. It is topologically equivalent to the two-dimensional sphere with unit radius in three dimensions, noted S^2. Therefore, pure states in two-level quantum systems can be represented by a unit

[4] The symplectic area is defined in an even manifold that is formed by pairs of directions: for example, symplectic areas in classical mechanics are specified in terms of position and momentum [72]. Here, we note that $2N-2$ free parameters describe the states in an N-dimensional complex Hilbert space (considering the global phase and the normalization), which accounts for the even number of dimensions.

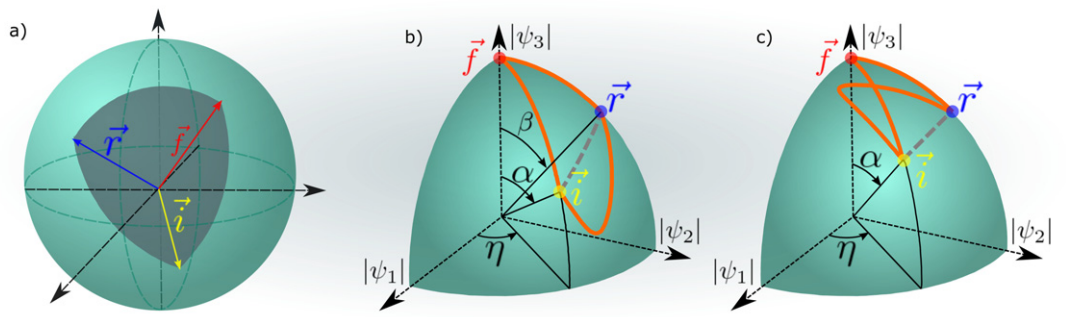

Figure 1. Representation of the geodesic triangle generated by the initial state ($\vec{i}$), the observable state ($\vec{r}$) and the final state ($\vec{f}$) in the complex projective spaces $\mathbb{C}\mathrm{P}^1$ (a) and $\mathbb{C}\mathrm{P}^2$ (b) and (c). The argument of the weak value of a projector is associated to the symplectic area of the triangle. (a) For two-level systems, the argument is also linked to the area and solid angle of the spherical triangle spanned by the three $\mathbb{R}^3$ vectors representing states on the Bloch sphere. (b) and (c) Depiction of two different geodesic triangles of three-level systems, using the spherical octant projection. Dashed gray lines represent great circle arcs connecting $\vec{i}$ and $\vec{r}$.

three-dimensional real vector $\vec{r}$ on the surface of the Bloch sphere. A two-level projector is then written in terms of the identity $\hat{I}$ and the traceless generators of SU(2), in this case the Pauli matrices $\hat{\vec{\sigma}} = (\hat{\sigma}_x, \hat{\sigma}_y, \hat{\sigma}_z)$, as $\hat{\Pi}_r = \frac{1}{2}\left(\hat{I} + \vec{r}\cdot\hat{\vec{\sigma}}\right)$. Using the properties of the Pauli matrices, the calculation of the weak value $\Pi_{r,w} = \mathrm{Tr}(\hat{\Pi}_f\hat{\Pi}_r\hat{\Pi}_i)/\,\mathrm{Tr}(\hat{\Pi}_f\hat{\Pi}_i)$ is straightforward [61]:

$$\Pi_{r,w} = \frac{1 + \vec{f}\cdot\vec{r} + \vec{r}\cdot\vec{i} + \vec{f}\cdot\vec{i} + \mathrm{i}\vec{f}\cdot\left(\vec{r}\times\vec{i}\right)}{\frac{1}{2}\left(1 + \vec{f}\cdot\vec{i}\right)}, \tag{2}$$

and the elegant formula resulting for the argument [61] is

$$\arg\,\Pi_{r,w} = \arctan\frac{\vec{f}\cdot\left(\vec{r}\times\vec{i}\right)}{1 + \vec{f}\cdot\vec{r} + \vec{r}\cdot\vec{i} + \vec{f}\cdot\vec{i}} = -\frac{\Omega_{irf}}{2}, \tag{3}$$

where $\vec{i}$ represents the pre-selected state and $\vec{f}$ the post-selected state, while $\vec{r}$ corresponds to the observable projector that is weakly probed. This purely geometric expression of the argument corresponds to minus one half of the solid angle Ω_{irf} intercepted on the Bloch sphere by the tetrahedron spanned from the three state vectors (where the path is followed in the order $i \to r \to f \to i$), as depicted in figure 1(a). Incidentally, we note that the numerator in (3) corresponds to twice the signed volume of this tetrahedron. When calculating the solid angle in (3), the signs of the numerator and denominator should be taken into account to determine the appropriate quadrant. The geodesics between quantum states correspond to arcs of great circles on the Bloch sphere. Thus, for two-level systems, the argument of the weak value of a projector corresponds to a solid angle [58, 59, 61], which is also equal to the surface of the Bloch sphere inside the geodesic triangle, i.e. to the area of a spherical triangle. Let us note that, using Stokes' theorem, the solid angle can be computed from any closed surface bounded by the geodesic triangle. It can thus be seen a contour integration along the geodesic path.

We now reformulate these insights by analyzing the argument of the Bargmann invariant $\mathrm{Tr}\,(\hat{\Pi}_f\hat{\Pi}_r\hat{\Pi}_i)$ [66] that appears in the numerator of the weak value expression $\Pi_{r,w}$. Because the denominator $\mathrm{Tr}\,(\hat{\Pi}_f\hat{\Pi}_i) = |\langle\psi_f|\psi_i\rangle|^2$ is always positive, the argument of the weak value is equal to the argument of the Bargmann invariant associated to the initial state, the projector state weakly measured and the final state [58, 59, 61, 67]. In any dimension, this invariant is linked to the geometric phase $\varphi_g = \arg\,\mathrm{Tr}(\hat{\Pi}_f\hat{\Pi}_r\hat{\Pi}_i) = \arg(\langle\psi_i|\psi_f\rangle\langle\psi_f|\psi_r\rangle\langle\psi_r|\psi_i\rangle)$ that would arise from a parametric evolution of the quantum system along the closed geodesic triangle (in the sequence $|\psi_i\rangle \to |\psi_r\rangle \to |\psi_f\rangle \to |\psi_i\rangle$) [56]:

$$\varphi_g = -\oint_{C_\Delta}\Im\langle\psi(s)|\frac{\mathrm{d}\psi(s)}{\mathrm{d}s}\rangle\,\mathrm{d}s = -2\iint_{\Sigma(C_\Delta)}\Im\langle\frac{\mathrm{d}\psi(s,t)}{\mathrm{d}t}|\frac{\mathrm{d}\psi(s,t)}{\mathrm{d}s}\rangle\,\mathrm{d}s\,\mathrm{d}t, \tag{4}$$

where we chose to describe states in Hilbert space for the convenience of readers familiar with the Hilbert space description of geometric phases. The first integral is the integral of the Berry connection along the closed geodesic triangle C_Δ parametrized by $|\psi(s)\rangle$. The last member of (4) is a surface integral over any closed surface $\Sigma(C_\Delta)$ bounded by the geodesic triangle C_Δ, where $|\psi(s,t)\rangle$ is an arbitrary parametrization

of the surface $\Sigma(C_\Delta)$. This is the integral of the Berry curvature. In any dimension, the argument of the weak value is thus identical to the Pancharatnam–Berry phase that a quantum state would pick up from a parametric state evolution along the closed geodesic triangle. We note however that weak values arise in many contexts in physics and we should not assume here that the geometric phase associated to the argument of the weak value is actually acquired by a quantum state evolving during the physical process described by the weak value.

The quantum state manifolds of N-level systems correspond to the complex projective spaces $\mathbb{C}\mathrm{P}^{N-1}$. They are Kähler manifolds [68], which means that they are equipped with a Hermitian form that provides both a Riemannian metric (Fubini–Study) and a symplectic form. The geometric phase (4) is linked to the symplectic area computed on the geodesic triangle using the symplectic form. In the qubit case, the Riemannian and symplectic areas of geodesic triangles are equivalent (they are equal up to a constant factor that depends on the normalization convention for the total areas). However, this is no longer the case in $\mathbb{C}\mathrm{P}^{N-1}$ with $N \geqslant 3$. For this reason, in three-level systems and beyond, the weak value argument cannot be as straightforwardly interpreted, nor as a solid angle, nor as a Riemannian area of a geodesic surface, as is possible in the qubit case. Nevertheless, the symplectic area is independent of the particular surface on which it is computed. The argument of the weak value of the projector is thus appropriately seen as arising from a contour integral along the boundary geodesics of the triangle, which accumulates the incremental geometric phase changes along the closed path. The argument of the weak value of any projector on pure state is a three-point invariant of the geodesic triangle.

We now generalize our geometric description to three-level systems. This is not trivial as the state manifold cannot be mapped bijectively to a (larger) sphere, contrary to the two-level case. In three-level systems, pure states are then associated with rays that are points of the projective plane $\mathbb{C}\mathrm{P}^2$. In $\mathbb{C}\mathrm{P}^1$, we used the identity and three (N^2-1 with $N=2$) 2×2 traceless generators of SU(2) (the three Pauli matrices) as a basis to expand the projectors. In $\mathbb{C}\mathrm{P}^2$, we expand projectors in terms of the eight (N^2-1 with $N=3$) 3×3 traceless Gell–Mann matrices $\hat{\lambda}_i$, a representation of the Lie algebra SU(3) [76] (we define the generators in appendix A). However, the quantum state manifold $\mathbb{C}\mathrm{P}^2$ is not equivalent to the surface of the seven-sphere S^7 in eight dimensions: all three-level states are on the sphere surface but most points on the surface of the seven-sphere are not proper quantum states. A projector on a pure state is

$$\hat{\Pi}_r = \frac{1}{3}\left(\hat{I} + \sqrt{3}\,\vec{r}\cdot\hat{\vec{\lambda}}\right), \tag{5}$$

where $\hat{\vec{\lambda}}$ is a vector whose components are the eight Gell–Mann matrices and $\vec{r}$ is an eight-dimensional, normalized[5], real vector [77, 78]. Additionally, the vector $\vec{r}$ must verify $\vec{r}\star\vec{r}=\vec{r}$, where the symmetric star product is defined by $(\vec{\alpha}\star\vec{\beta})_c = \sqrt{3}d_{abc}\alpha_a\beta_b$ [77, 78] (the components $a,b,c\in\{1,2,\ldots,8\}$ and Einstein's summation convention is assumed for repeated indices). The constants d_{abc} are completely symmetric under index permutation and arise from the anti-commutator of the generators of the of SU(3) Lie algebra: they are determined by $d_{abc} = \frac{1}{4}\,\mathrm{Tr}(\hat{\lambda}_a\{\hat{\lambda}_b,\hat{\lambda}_c\})$. The star product condition ensures that the vector $\vec{r}$ on the unit seven-sphere also corresponds to a point of $\mathbb{C}\mathrm{P}^2$ (hence represents a pure quantum state). This condition comes by imposing that the square of the projector should be equal to the projector itself (see appendix B). The star product appears in a few papers in the literature [71, 77–82] but not many (to our knowledge). We would like to stress that many familiar properties of the SU(2) Bloch sphere do not hold in larger dimensions. For example, the eight-dimensional vectors representing orthogonal states of a three-level system form angles of 120° (on the Bloch sphere, two vectors associated to orthogonal states are opposite, that is form 180° angles). Therefore, the three vectors of a basis are in a plane with 120° between them. Also, there is no equivalent of the $\star$ product in SU(2). For this reason, we discuss a few essential properties of the state representation as generalized Bloch spheres in appendices D and E to provide more context for the interested reader.

We use the properties of the generators of the Lie algebra of SU(3) to calculate the expression of the weak value of a three-level system projector from (1): $\Pi_{r,w} = \mathrm{Tr}\,(\hat{\Pi}_f\hat{\Pi}_r\hat{\Pi}_i)\,/\,\mathrm{Tr}\,(\hat{\Pi}_f\hat{\Pi}_i)$. Applying the definition of projectors in terms of Gell–Mann matrices (5), we find

$$\Pi_{r,w} = \frac{1 + 2\vec{f}\cdot\vec{r} + 2\,\vec{r}\cdot\vec{i} + 2\vec{f}\cdot\vec{i} + 2\vec{f}\cdot\left(\vec{r}\star\vec{i}\right) + \mathrm{i}\,2\sqrt{3}\vec{f}\cdot\left(\vec{r}\wedge\vec{i}\right)}{3 + 6\vec{f}\cdot\vec{i}}, \tag{6}$$

where the eight-dimensional real vectors $\vec{i}$, $\vec{f}$ and $\vec{r}$ represent the pre- and post-selected states and the weakly measured projector state, respectively. In addition to the previously defined star product, we also introduced

[5] In this work, we chose the convention to work with normalized vectors on a single unit sphere. See appendix B for more details.

the antisymmetric wedge product [77, 80, 82] $(\vec{\alpha}\wedge\vec{\beta})_c = f_{abc}\alpha_a\beta_b$, with $f_{abc} = -\frac{1}{4}\mathrm{i}\ \mathrm{Tr}(\hat{\lambda}_a[\hat{\lambda}_b,\hat{\lambda}_c])$, the structure constants of the Lie algebra of SU(3) (which are completely anti-symmetric under index permutations and emerge from the commutator of the generators of the Lie algebra). Note that the $\star$ and $\wedge$ products produce vectors that are both outside of $\mathbb{C}\mathrm{P}^2$ and not normalized in general (so they do not represent states). The vector $\vec{\alpha}\wedge\vec{\beta}$ produced by the wedge product is orthogonal to the two initial vectors $\vec{\alpha}$ and $\vec{\beta}$. Also, the two products are orthogonal: for any pre- and post-selected states $(\vec{i}\wedge\vec{f})\cdot(\vec{i}\star\vec{f}) = 0$. In (6), the two scalar products $\vec{f}\cdot(\vec{r}\star\vec{i})$ and $\vec{f}\cdot(\vec{r}\wedge\vec{i})$ are invariants under cyclic permutations of the three vectors and under unitary transformations. The qutrit weak value (6) bears similarities with the qubit case (2): for SU(2), the structure constants f_{abc} are given by the Levi-Civita symbol while $d_{abc} = 0$, so that the wedge product reduces to the usual cross-product in three dimensions while the star product contribution disappears. We discuss additional properties of the $\star$ and $\wedge$ products in appendix D and we provide detailed calculations leading to (6) in appendix C (although we recommend skipping the latter for now).

Weak values are regularly considered in terms of their real and imaginary parts because this is how they affect typical weak measurements. Nonetheless, interpreting weak values in terms of their modulus and argument provides us more insight about their geometrical properties. Considering the real and imaginary parts of (6), the weak value argument is,

$$\arg\,\Pi_{r,w} = \arctan\frac{2\sqrt{3}\vec{f}\cdot\left(\vec{r}\wedge\vec{i}\right)}{1+2\left(\vec{f}\cdot\vec{r}+\vec{r}\cdot\vec{i}+\vec{f}\cdot\vec{i}\right)+2\vec{f}\cdot\left(\vec{r}\star\vec{i}\right)} + \phi\left(\Pi_{r,w}\right), \tag{7}$$

where the term ϕ essentially determines the appropriate quadrant (the quadrant depends on the signs of the real and imaginary parts of the weak value):

$$\phi(f) = \begin{cases} 0 \text{ if } \Re(f) > 0 \\ \pi \text{ if } \Re(f) < 0 \end{cases}. \tag{8}$$

As discussed previously, this argument represents a geometric phase because it is equal to the argument of the Bargmann invariant [66] associated to the initial state, the projector state weakly measured and the final state [58, 59, 61, 67] as expressed in (4). It corresponds to a symplectic area evaluated on the geodesic triangle using the symplectic form of the projective space $\mathbb{C}\mathrm{P}^2 = \mathrm{SU}(3)/\mathrm{U}(2)$ [77], whose expression depends only on the vertices $\vec{i}$, $\vec{r}$ and $\vec{f}$ (which confirms the purely geometric origin of the argument). It is important to note that the geodesics of the quantum state manifold do not correspond to geodesics of S^7: they are not arcs of great circles of S^7. In particular, the geometric phase is not equivalent to the Riemannian area of the S^7 spherical triangle defined by the three vertices (which could include points that are not states), nor to the Riemannian area of a surface built from geodesics linking one vertex to the opposite side of the geodesic triangle (which is not unique as the surface generally depends on the chosen vertex in the triangle).

In figure 1, we represent the geodesic triangle spanned by three quantum states associated to a projector weak value, in $\mathbb{C}\mathrm{P}^1$ for qubit systems and in $\mathbb{C}\mathrm{P}^2$ for qutrit systems. For two-level systems, the three quantum states lay on the surface of the Bloch sphere and the argument is connected to the area of the spherical triangle, equivalent to the solid angle. For three-level systems, the geometry is more complicated. Most generally, we can represent $\mathbb{C}\mathrm{P}^2$ graphically using a three-dimensional sphere octant, where each point is furthermore associated to a torus linked to the two phase components χ_2 and χ_3 of the state vector in Hilbert space [68, 77]: $|\psi\rangle = \left(|\psi_1|\mathrm{e}^{\mathrm{i}\chi_1}, |\psi_2|\mathrm{e}^{\mathrm{i}\chi_2}, |\psi_3|\right)^{\mathrm{T}}$. Each state $|\psi\rangle$ is projected on the sphere octant on the point with (real) coordinates $\vec{q} = \left(|\psi_1|, |\psi_2|, |\psi_3|\right)^{\mathrm{T}}$. Considering the invariance under unitary transformations, the most general geodesic triangle can be represented by the states $|f\rangle = (0,0,1)^{\mathrm{T}}$, $|r\rangle = (0, \sin\beta, \cos\beta)^{\mathrm{T}}$ and $|i\rangle = \left(\sin\alpha\cos\eta, \mathrm{e}^{\mathrm{i}\chi_2}\sin\alpha\sin\eta, \cos\alpha\right)^{\mathrm{T}}$, as depicted in figure 1. Beware that the geodesics connecting the triangle vertices on the octant do not typically appear as spherical arcs. Each pair of vertices generates a unique complex projective line (i.e. a two dimensional subspace isomorphic to a Bloch sphere) in the complex projective plane $\mathbb{C}\mathrm{P}^2$. Topologically, the three geodesics connecting the vertices are thus arcs of great circles in each of these three distinct (in general) $\mathbb{C}\mathrm{P}^1$ subspaces. However, when projected on the sphere octant, the geodesic triangle is inevitably distorted. On the S^7 sphere, these geodesics would appear as circle arcs connecting the vertices. However these circle arcs would not be arcs of great circles because the geodesics of $\mathbb{C}\mathrm{P}^2$ are not those of S^7 (which is a reminder that the points of $\mathbb{C}\mathrm{P}^2$ are constrained to a four-dimensional subspace of S^7 equipped with the Fubini–Study metric and not with the metric of the round sphere). The general expression of a state on S^7 and of the geodesic arc linking $\vec{r}$ and $\vec{f}$ are given in appendix E for reference.

3. Weak values of projectors in $\mathbb{C}^N$

Our results on three-level systems can be easily generalized to N-level systems. Projectors on pure states in $\mathbb{C}^N$ are associated with straight complex lines passing through the origin or, equivalently, with rays that are points of the projective space $\mathbb{C}\mathrm{P}^{N-1}$. We describe them in terms of the N^2-1 generators of the Lie algebra of SU(N) that generalize the Pauli and Gell–Mann matrices (see appendix A for details). In that case, a projector on a pure state is (see appendix B)

$$\hat{\Pi}_r = \frac{1}{N}\hat{I}_N + \sqrt{\frac{N-1}{2N}}\,\vec{r}\cdot\hat{\vec{L}}, \tag{9}$$

where $\hat{\vec{L}}$ is a vector whose N^2-1 components give the generators $\hat{L}_a$. The real vector $\vec{r}$ has also N^2-1 components. It is normalized ($\vec{r}\cdot\vec{r}=1$), so that the state is on the surface of the S^{N^2-2} sphere in N^2-1 dimensions. Additionally it is constrained to a subspace of this sphere by the extra condition $\vec{r}\star\vec{r}=\vec{r}$, where the star product is defined by $(\vec{q}\star\vec{r})_c = \sqrt{\frac{N(N-1)}{2}}\frac{1}{N-2}d_{abc}q_a r_b$ [81], with the symmetric constants of SU(N) given from the anti-commutator by $d_{abc} = \frac{1}{4}\,\mathrm{Tr}(\hat{L}_a\{\hat{L}_b,\hat{L}_c\})$ as previously. This constraint ensures that the point $\vec{r}$ on the sphere corresponds to a projector on a pure state and, thus, is associated to a proper quantum pure state belonging to $\mathbb{C}\mathrm{P}^{N-1}$. As for qutrit systems, this condition makes it impossible to describe the geometry of the states as the complete surface of a sphere: the pure quantum states belong to a $(2N-2)$-dimensional subspace of the S^{N^2-2} sphere. In this space, when two quantum states $|\psi\rangle$ and $|\phi\rangle$ are orthogonal, the vectors $\vec{r}_\psi$ and $\vec{r}_\phi$ representing those states on the generalized Bloch sphere form an angle of $\pi - \arccos\frac{1}{N-1}$. In the limit of very large N, the angle between the vectors associated to orthogonal states tends to 90°. In appendix B, we provide context to our definition of the symmetric $\star$ product in SU(N) as a generalization of its original SU(3) definition [77, 78].

The argument of the weak value of a projector $\hat{\Pi}_r$ on a pure state of an N-level system is expressed using the properties of the generators of SU(N) as,

$$\arg\,\Pi_{r,w} = \arctan\frac{2\left(\frac{N-1}{2N}\right)^{\frac{3}{2}}\vec{f}\cdot\left(\vec{r}\wedge\vec{i}\right)}{\frac{1}{N^2}+\frac{N-1}{N^2}\left(\vec{f}\cdot\vec{r}+\vec{r}\cdot\vec{i}+\vec{f}\cdot\vec{i}\right)+\frac{(N-1)(N-2)}{N^2}\vec{f}\cdot\left(\vec{r}\star\vec{i}\right)} + \phi\left(\Pi_{r,w}\right), \tag{10}$$

where $\phi\left(\Pi_{r,w}\right)$ selects the appropriate quadrant and is specified in (8). Detailed calculations leading to (10) are provided in appendix C. The anti-symmetric wedge product is defined similarly to the qutrit case using the structure constants of SU(N), which are obtained from the commutation relationships of the generators: $f_{abc} = -\frac{1}{4}\mathrm{i}\,\mathrm{Tr}(\hat{L}_a[\hat{L}_b,\hat{L}_c])$. It produces the vector with components $(\vec{\alpha}\wedge\vec{\beta})_c = f_{abc}\alpha_a\beta_b$, which is orthogonal to both $\vec{\alpha}$ and $\vec{\beta}$. The expression (10) of the argument of the weak value generalizes the one obtained for three-level systems (7) to the case of N-level system projectors on pure states. Taking $N=3$ and $N=2$, we recover the results for three-level system projectors and qubit systems, respectively. As explained previously, the argument of the weak value of a projector is equal to the argument of the Bargmann invariant of the three states involved. Therefore, the argument (10) represents a geometric phase connected to the symplectic area of the geodesic triangle in $\mathbb{C}\mathrm{P}^{N-1}$.

To conclude this section, we first would like to emphasize that, using an appropriate unitary transformation, any set of three states of $\mathbb{C}\mathrm{P}^{N-1}$ and the geodesics linking them can always be mapped to a $\mathbb{C}\mathrm{P}^2$ subspace. Therefore, all observations valid for the weak value of qutrit projectors on pure states extend to arbitrary larger dimensions. In particular, figure 1 provides a valid representation of geodesic triangles in $\mathbb{C}\mathrm{P}^{N-1}$. Furthermore, from a geometric point of view, all weak values of projectors in any finite dimension can be described using eight-dimensional, normalized real vectors using the formulas (6) and (7) valid for $\mathbb{C}\mathrm{P}^2$. We also note that there are two three-point invariants that contribute to the geometric phase: $\vec{f}\cdot(\vec{r}\wedge\vec{i}) = f_{abc}f_a r_b i_c$ and $\vec{f}\cdot(\vec{r}\star\vec{i}) = \sqrt{\frac{N(N-1)}{2}}\frac{1}{N-2}d_{abc}f_a r_b i_c$. Both are invariant under cyclic permutations of the three vectors and under unitary transformations. However, the former is anti-symmetric under the permutation of two vectors, while the latter is symmetric.

4. Weak values of general observables

Weak measurement are not confined to projectors on pure states. In practice, experiments also deal with the weak values of arbitrary observables, such as the spin of a particle, projectors on degenerate subspaces or compound observables in multipartite systems to name a few. In this section, we study the weak value of a

general Hermitian observable $\hat{A}$ of an N-level system. We will show that the weak value of any observable can be expressed in terms of the weak value of a very specific projector that will provide us with a geometrical description in the spirit of what we did before. We decompose the observable in terms of the $N \times N$ identity operator and a traceless operator from SU(N):

$$\hat{A} = a_I \hat{I}_N + a_L \vec{\alpha} \cdot \hat{\vec{L}}, \tag{11}$$

where $\hat{\vec{L}}$ is a vector whose $N^2 - 1$ components are the generators of the SU(N) Lie group (see appendix A), a_I and a_L are real constants and $\vec{\alpha}$ is a normalized vector with $N^2 - 1$ real components. Using the properties of the generators $\hat{\vec{L}}$ to compute the traces appearing in the definition (1), we obtain the weak value of a general observable (as shown in appendix C):

$$A_{\alpha,w} = \frac{1}{\frac{1}{N} + \frac{N-1}{N}\vec{f}\cdot\vec{i}}\left[\mathrm{i}\frac{a_L(N-1)}{N}\vec{f}\cdot\left(\vec{\alpha}\wedge\vec{i}\right) + \frac{a_I}{N} + \frac{a_I(N-1)}{N}\vec{f}\cdot\vec{i} + \frac{a_L\sqrt{2(N-1)}}{N\sqrt{N}}\left(\vec{f}\cdot\vec{\alpha} + \vec{\alpha}\cdot\vec{i}\right)\right.$$
$$\left. + \frac{a_L\sqrt{2(N-1)}(N-2)}{N\sqrt{N}}\vec{f}\cdot\left(\vec{\alpha}\star\vec{i}\right)\right]. \tag{12}$$

This expression generalizes our previous results on projectors, which we recover by setting the appropriate coefficients a_I and a_L from (9) and by constraining the operator using $\vec{\alpha} = \vec{\alpha}\star\vec{\alpha}$. It is thus crucial to note that, in (12), the vectors $\vec{i}$ and $\vec{f}$ must obey the constraints $\vec{i} = \vec{i}\star\vec{i}$ and $\vec{f} = \vec{f}\star\vec{f}$ because they represent states, while $\vec{\alpha}$ is allowed to range freely on the whole surface of the S^{N^2-2} sphere (for this reason, we denote the latter vector with a Greek letter, while the former are identified by roman letters). Our normalization conventions for the projector definition (9) allowed us to express the weak values in terms of the geometrical properties of three vectors that all belong to the same unit sphere (see appendix B).

By considering the ratio of the imaginary and real parts of (12), we find the argument of the weak value of an arbitrary Hermitian observable:

$$\arg\left(A_{\alpha,w}\right) = \phi\left(A_{\alpha,w}\right) + \arctan\frac{\frac{a_L(N-1)}{N}\vec{f}\cdot\left(\vec{\alpha}\wedge\vec{i}\right)}{\frac{a_I}{N} + \frac{a_I(N-1)}{N}\vec{f}\cdot\vec{i} + \frac{a_L\sqrt{2(N-1)}}{N\sqrt{N}}\left(\vec{f}\cdot\vec{\alpha} + \vec{\alpha}\cdot\vec{i}\right) + \frac{a_L\sqrt{2(N-1)}(N-2)}{N\sqrt{N}}\vec{f}\cdot\left(\vec{\alpha}\star\vec{i}\right)}, \tag{13}$$

where $\phi\left(A_{\alpha,w}\right)$ specifies the quadrant according to (8). This expression bears similarities to the argument of the weak value of a projector on a pure state (10). Notwithstanding the appearance of the constant factors a_I and a_L, the essential differences are the new term a_I/N in the denominator and the fact that $\vec{\alpha}$ does not represent a state in general. We notice that the numerator is fully antisymmetric under permutations of vectors, while the denominator is symmetric under permutations of the initial and final states. The term involving the star product is even fully symmetric under permutations of the three vectors.

In order to interpret this argument in terms of a geometric phase, we relate it to the weak value of a particular projector on a pure state (we call it $\hat{\Pi}_{i'}$). This approach allows us to link the argument to the Bargmann invariant of the pre-selected state, the projector $\hat{\Pi}_{i'}$ and the post-selected state, and, therefore, to a symplectic area in $\mathbb{C}\mathrm{P}^{N-1}$. We define this projector by

$$\hat{\Pi}_{i'} = \frac{\hat{A}|\psi_i\rangle\langle\psi_i|\hat{A}}{\langle\psi_i|\hat{A}^2|\psi_i\rangle} \tag{14}$$

when $\hat{A}|\psi_i\rangle \neq 0$ (else the weak value is 0 and the argument is undefined anyway). The state $|\psi_{i'}\rangle$ results from the application of the observable to the initial state. Since the argument of the weak value of a projector is equal to the argument of the Bargmann invariant, we have

$$\arg\,\Pi_{i',w} = \arg[\mathrm{Tr}\,(\hat{\Pi}_f\hat{\Pi}_{i'}\hat{\Pi}_i)] = \arg\,\frac{\langle\psi_f|\hat{A}|\psi_i\rangle\langle\psi_i|\hat{A}|\psi_i\rangle\langle\psi_i|\psi_f\rangle}{\langle\psi_i|\hat{A}^2|\psi_i\rangle}. \tag{15}$$

The expectation value of $\hat{A}^2$ in the pre-selected state is strictly positive and does not contribute to the total argument: $\arg\langle\psi_i|\hat{A}^2|\psi_i\rangle = 0$. The average value $\langle A\rangle_{\psi_i} = \langle\psi_i|\hat{A}|\psi_i\rangle$ is a real number: its argument is 0 if it is positive and π if it is negative. Hence, the argument of the weak value of the observable $\hat{A}$ is equivalent to the argument of the weak value of the projector $\hat{\Pi}_{i'}$ modulo π:

$$\arg\,A_w = \arg\,\Pi_{i',w} - \arg\,\langle A\rangle_{\psi_i}. \tag{16}$$

We find two contributions. First, the geometric phase arising from the geodesic triangle in $\mathbb{C}\mathrm{P}^{N-1}$ whose vertices correspond to the vectors $\vec{i}$, $\vec{i}'$ and $\vec{f}$ on the S^{N^2-2} sphere. It is connected to the symplectic area of the geodesic triangle and can alternatively be computed from (4). Second, another geometric phase that is given by the sign of average value of the observable in the initial state. It can easily be expressed in the present formalism, on S^{N^2-2}, in terms of the vectors $\vec{i}$ and $\vec{\alpha}$ by setting $\vec{i}=\vec{f}$ in (12), as done later in section 8 with (31).

Describing geometrically the relationship existing between an arbitrary initial state $|\psi_i\rangle$ and the quantum state associated to the projector $\hat{\Pi}_{i'}$ produced by an observable $\hat{A}$ according to (14) is far from a trivial task in general. In the case of the Pauli observables $\vec{\alpha}\cdot\hat{\vec{\sigma}}$, the vector $\vec{i}'$ corresponds to the mirror image of the initial state $\vec{i}$ with respect to the axis $\vec{\alpha}$ of the Pauli operator (i.e. the direction of the spin measurement). However, these particular observables are also unitary operators, which helps in determining their action on a general initial state. More complicated operators or families of operators should be studied on case by case basis. Subsequently in this paper, we will consider in depth the situation of general observables of two-level systems and leave most higher dimensional cases for follow-up studies.

When the average value $\langle A\rangle_{\psi_i}$ equals zero, its argument can be 0 or π in (16). In this case, the projectors $\hat{\Pi}_i$ and $\hat{\Pi}_{i'}$ are also orthogonal. Therefore, they are linked by infinitely many geodesics and, at first, it is not clear how to define the geodesic triangle. However, the argument of the weak value on the left-hand side of (16) is well-defined since we assumed $A_w\neq 0$. This indicates that it is possible to select an appropriate geodesic to construct the geodesic triangle. This can be done by computing the limit of a family of geodesic triangles built from slightly perturbing the initial state $\hat{\Pi}_i=\lim_{\epsilon\to 0}\hat{\Pi}_i(\epsilon)$ so that $\mathrm{Tr}\,\hat{A}\,\hat{\Pi}_i(\epsilon)=\langle A\rangle_{\psi_i(\epsilon)}\neq 0$. There will be two choices for the geodesic (arising from the cases $\langle A\rangle_{\psi_i(\epsilon)}>0$ and $\langle A\rangle_{\psi_i(\epsilon)}<0$) that will give the correct value for the argument of the weak value using (16). Note that evaluating this limit would often occur automatically when studying the geodesic triangle as a function of the initial state (a natural use of the formalism). Alternatively, it is also possible to work with the projector $\hat{\Pi}_{f'}$ defined from the application of the operator on the post-selected state $\hat{A}|\psi_f\rangle$ (assuming $\langle A\rangle_{\psi_f}\neq 0$).

5. Weak values of the generators of the Lie group of SU(N)

As a relevant, direct application of the results obtained in the previous section, we express the weak values of the generators of the Lie algebra of SU(2) (Pauli matrices), SU(3) (Gell–Mann matrices) and SU(N) in general. Operators linked to these generators describe the spin of particles, light polarization, the orbital angular momentum of light and the polarization correlations in entangled photons, to cite the most typical laboratory use. They are also related to observables in particle physics and cosmology, where conceptual applications of weak measurements start to emerge [83]. We obtain the weak value and its argument, of all the generators, by setting $a_I=0$ and $a_L=1$ in the expressions (12) and (13), respectively.

First, we recover the weak value and its argument for two-level systems ($N=2$) [84], which are useful points of comparison:

$$\sigma_{r,w}=\frac{\vec{f}\cdot\vec{r}+\vec{r}\cdot\vec{i}+\mathrm{i}\left[\vec{f}\cdot\left(\vec{r}\times\vec{i}\right)\right]}{1+\vec{f}\cdot\vec{i}}, \tag{17}$$

$$\arg\,\sigma_{r,w}=\arctan\frac{\vec{f}\cdot\left(\vec{r}\times\vec{i}\right)}{\vec{f}\cdot\vec{r}+\vec{r}\cdot\vec{i}}+\phi\left(\sigma_{r,w}\right), \tag{18}$$

where $\phi\left(\sigma_{r,w}\right)$ is defined in (8) and the generator is given by $\vec{r}\cdot\hat{\vec{\sigma}}$. In the particular case of SU(2), the star product is null and wedge product is equivalent to the cross product because the structure constants f_{abc} become the Levi-Civita symbol. Additionally, the vector $\vec{r}$ also represents a state and it is then possible to show that (18) is given by the sum of two solid angles connected to two Bargmann invariants [84]. These two solid angles correspond to the two contributions found in (16) when using the projector $\hat{\Pi}_{i'}$ to determine the geometric phase.

Second, we consider the generators $\vec{\alpha}\cdot\hat{\vec{\lambda}}$ of the Lie group SU(3), i.e. the Gell–Mann matrices [76]:

$$\lambda_{\alpha,w}=\frac{2}{\sqrt{3}}\frac{\vec{f}\cdot\vec{\alpha}+\vec{\alpha}\cdot\vec{i}+\vec{f}\cdot\left(\vec{\alpha}\star\vec{i}\right)+\sqrt{3}\,\mathrm{i}\vec{f}\cdot\left(\vec{\alpha}\wedge\vec{i}\right)}{1+2\vec{f}\cdot\vec{i}}, \tag{19}$$

$$\arg\,\lambda_{\alpha,w}=\arctan\frac{\sqrt{3}\vec{f}\cdot\left(\vec{\alpha}\wedge\vec{i}\right)}{\vec{f}\cdot\vec{\alpha}+\vec{\alpha}\cdot\vec{i}+\vec{f}\cdot\left(\vec{\alpha}\star\vec{i}\right)}+\phi\left(\lambda_{\alpha,w}\right), \tag{20}$$

with $\phi(\lambda_{\alpha,w})$ defined in (8) and where $\vec{\alpha}$ does not represent a state in general. We note the elegant similarities between the weak values of qubit and qutrit systems. However, the complexity introduced in particular by the additional term involving the star product makes it no longer possible to interpret straightforwardly the geometric phase (20). Indeed, in addition to the three initial vectors $\vec{i}$, $\vec{\alpha}$ and $\vec{f}$, we also have to consider the directions of $\vec{f}\wedge\vec{\alpha}$ and $\vec{f}\star\vec{\alpha}$, which prevent us from reducing the problem to the three dimensions spanned by $\vec{i}$, $\vec{\alpha}$ and $\vec{f}$.

Third, for the generators $\vec{\alpha}\cdot\hat{\vec{L}}$ of SU(N) generalizing the Pauli and Gell–Mann matrices, the weak value and its argument are

$$L_{\alpha,w}=\sqrt{2\frac{N-1}{N}}\frac{\vec{f}\cdot\vec{\alpha}+\vec{\alpha}\cdot\vec{i}+(N-2)\vec{f}\cdot\left(\vec{\alpha}\star\vec{i}\right)+\mathrm{i}\sqrt{\frac{N^2-N}{2}}\vec{f}\cdot\left(\vec{\alpha}\wedge\vec{i}\right)}{1+(N-1)\vec{f}\cdot\vec{i}}, \tag{21}$$

$$\arg L_{\alpha,w}=\arctan\frac{\sqrt{\frac{1}{2}N(N-1)}\,\vec{f}\cdot\left(\vec{\alpha}\wedge\vec{i}\right)}{\vec{f}\cdot\vec{\alpha}+\vec{\alpha}\cdot\vec{i}+(N-2)\,\vec{f}\cdot\left(\vec{\alpha}\star\vec{i}\right)}+\phi\left(L_{\alpha,w}\right), \tag{22}$$

with $\phi(L_{\alpha,w})$ defined in (8).

6. Weak value of a two-level system observable

We turn our attention to the weak values of arbitrary observables in two-level systems. In particular, we are interested in analyzing their connection to the projector $\hat{\Pi}_{i'}$ (14) that characterizes the geometric phase associated to their argument (16). Advantageously, all operators and states of two level systems are linked to a unit vector on the Bloch sphere. We note the initial and final states $\vec{i}$ and $\vec{f}$. Without loss of generality, we consider an observable of the form (11), written as

$$\hat{O}_r=a\left(\hat{I}+\gamma\,\vec{r}\cdot\hat{\vec{\sigma}}\right), \tag{23}$$

where $\vec{r}$ is a unit vector and a and γ are real constants. Later on, γ will appear as the relevant parameter for studying geometric phases. When $\gamma=0$, the weakly measured observable is the identity. When $\gamma=1$, it is proportional to a projector. Then, when $\gamma\to\infty$, it tends to a linear combination of the Pauli matrices, proportional to $\vec{r}\cdot\hat{\vec{\sigma}}$. From (12) and (13), we readily obtain the weak value and its argument:

$$O_{r,w}=a\frac{1+\vec{f}\cdot\vec{i}+\gamma\left(\vec{f}\cdot\vec{r}+\vec{r}\cdot\vec{i}\right)+\mathrm{i}\gamma\vec{f}\cdot\left(\vec{r}\times\vec{i}\right)}{1+\vec{f}\cdot\vec{i}}, \tag{24}$$

$$\arg O_{r,w}=\arctan\frac{\gamma\vec{f}\cdot\left(\vec{r}\times\vec{i}\right)}{1+\vec{f}\cdot\vec{i}+\gamma\left(\vec{f}\cdot\vec{r}+\vec{r}\cdot\vec{i}\right)}+\phi\left(O_{r,w}\right), \tag{25}$$

with $\phi(O_{r,w})$ giving the appropriate quadrant for the argument, on the basis of the sign of the real part of the weak value (8). It should be highlighted that the argument of the weak value depends chiefly on γ. The parameter a only contributes a 0 or π term through $\phi(O_{r,w})$, depending on its sign. Interestingly, the parameter γ plays a role similar to a measurement strength, from which the geometric phase (25) emerges [65].

The projector $\hat{\Pi}_{i'}=\hat{O}_r\hat{\Pi}_i\hat{O}_r/\operatorname{Tr}\hat{\Pi}_i\hat{O}_r^2$ (14) connects the geometric phase (25) to the argument of a Bargmann invariant. Its Bloch sphere vector is

$$\vec{i}'=\frac{1}{1+2\gamma\,\vec{r}\cdot\vec{i}+\gamma^2}\left[\left(1-\gamma^2\right)\vec{i}+2\gamma\left(1+\gamma\,\vec{r}\cdot\vec{i}\right)\vec{r}\right]. \tag{26}$$

Figure 2 depicts the evolution of the $\vec{i}'$ vector as a function of the observable parameter γ. When $\gamma=0$, $\vec{i}'$ is the pre-selected state $\vec{i}$ because the observable is the identity. With $\gamma=1$, $\vec{i}'$ corresponds to $\vec{r}$ since for that value of γ, the operator itself is already a projector. When $\gamma\to\infty$, the observable is proportional to the Pauli operator $\vec{r}\cdot\hat{\vec{\sigma}}$. Then, $\vec{i}'$ is the mirror image $\vec{i}_m$ of the initial vector $\vec{i}$ with respect to the direction $\vec{r}$ [84]:

$$\vec{i}_m=-\vec{i}+2\left(\vec{i}\cdot\vec{r}\right)\vec{r}. \tag{27}$$

All the possible locations of $\vec{i}'$ form the great circle that connects the initial state $\vec{i}$ to the direction $\vec{r}$ associated to the operator. Positive values of γ correspond to the arc linking $\vec{i}\to\vec{r}\to\vec{i}_m$, while the negative

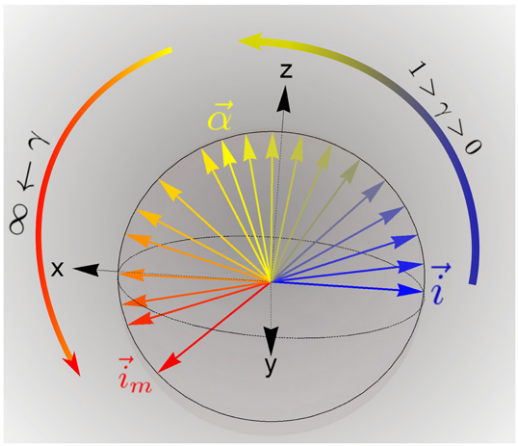

Figure 2. Representation of the vector $\vec{i}'$ on the Bloch sphere for positive values of the parameter γ. The blue vector is the initial state, the yellow vector is the vector $\vec{r}$ associated to the observable. The red vector $\vec{i}_m$ is the mirror image of the initial state with respect to the vector $\vec{r}$.

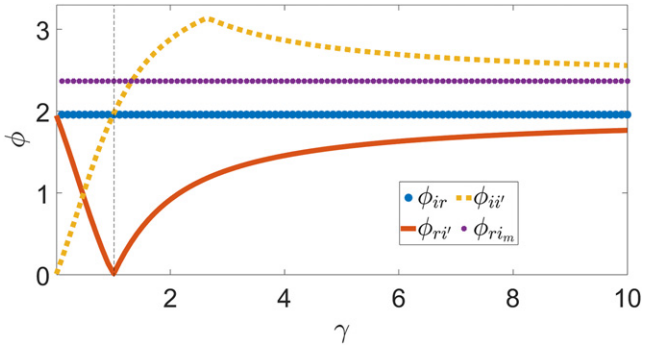

Figure 3. Evolution of the smallest angles subtended by the four vectors $\vec{i}$ (arbitrary initial state), $\vec{r}$ (vector associated to the arbitrary qubit operator $\hat{O}_r$), $\vec{i}_m$ (mirror image of $\vec{i}$ through the direction $\vec{r}$) and $\vec{i}'$ (Bloch sphere direction giving the geometric phase associated to the weak value as half a solid angle). In yellow: the angle $\phi_{ii'}$ between $\vec{i}$ and $\vec{i}'$. In dark orange: the angle $\phi_{ri'}$ between $\vec{r}$ and $\vec{i}'$. In blue and purple: the constant angles ϕ_{ir} and $\phi_{ri_m} = 2(\pi - \phi_{ir})$, between $\vec{i}$ and $\vec{r}$ and between $\vec{r}$ and $\vec{i}_m$, respectively.

values of gamma give the complementary arc $\vec{i} \to -\vec{r} \to \vec{i}_m$. Knowing $\vec{i}'$, it becomes possible to represent geometrically the argument of the weak value on the Bloch sphere, as a function of γ for fixed pre- and post-selected states, in a manner similar to figure 1(a). This is the main appeal of this projector.

At a more quantitative level, figure 3 represents the smallest angles existing between the various relevant vectors. Two angles are constant: ϕ_{ir} between the initial state $\vec{i}$ and the operator vector $\vec{r}$, as well as ϕ_{ii_m} between the initial state and its mirror image $\vec{i}_m$ through $\vec{r}$. The evolution of the angle $\phi_{ii'}$ between the initial state $\vec{i}$ and the projector $\vec{i}'$ goes from 0 for $\gamma = 0$ (when the operator is the identity), to ϕ_{ir} for $\gamma = 1$ (when the operator $\hat{O}_r$ is the projector on $\vec{r}$), to the maximum value of π for $\gamma = -1/\cos\phi_{ir}$. The latter corresponds to $\hat{O}_r|\psi_i\rangle = 0$. In this case, both the weak value $O_{r,w}$ and the average value $\langle O_r\rangle_{\psi_i}$ are null, and the argument of the weak value is undefined. This value of γ delimits the parameter ranges for which the average value contributes a factor 0 or π to the geometric phase (16), according to its sign. Beyond this critical value of γ, the value of the $\phi_{ii'}$ angle decreases and tends to ϕ_{ii_m}. We also see that the angle $\phi_{ri'}$ between $\vec{r}$ and $\vec{i}'$ is equal to ϕ_{ir} when $\gamma = 0$ or $\gamma \to \infty$, as these limiting cases correspond to mirror images with respect to $\vec{r}$. When the operator is a projector ($\gamma = 1$), $\phi_{ri'} = 0$. Finally, we observe that $\phi_{ii'}$ parametrizes the longitude along the great circle arc described by $\vec{i}'$. $\phi_{ii'}$ can be expressed solely in terms of ϕ_{ir} and γ by projecting (26) on the initial state.

7. Projectors on degenerate subspaces and Hermitian quantum gates

Sections 2 and 3 dealt with the weak values of projectors on pure states. However, projectors on degenerate subspaces also arise in practice. For example, the square of a spin-1 operator is associated to a doubly

degenerate subspace, which plays an essential role in proofs of quantum contextuality [85]. As shown in appendix B, an arbitrary projector $\hat{P}$ on a k-degenerate subspace of $\mathbb{C}^n$ takes the form

$$\hat{P} = \frac{k}{N}\hat{I}_N + \sqrt{\frac{k(N-k)}{2N}}\vec{\rho}\cdot\vec{L}, \tag{28}$$

where the normalized, real vector $\vec{\rho}$ on the S^{N^2-2} sphere is constrained by the star product according to

$$\vec{\rho}\star\vec{\rho} = \frac{N-2k}{N-2}\sqrt{\frac{N-1}{k(N-k)}}\vec{\rho}. \tag{29}$$

Setting $k=1$ in (28) and (29), we recover the projectors on pure states. Then, $\vec{\rho}$ is associated to a quantum state in $\mathbb{C}\mathrm{P}^{N-1}$, but not otherwise (see example in appendix B).

The specific expressions of the weak value and its argument can be deduced as a straightforward application of (12) and (13). The point we actually wish to stress here is that, for such observables, the projector $\hat{\Pi}_{i'}$ (16) of $\mathbb{C}\mathrm{P}^{N-1}$, whose argument of the Bargmann invariant with the pre- and post-selected states is linked to the weak value geometric phase, has a straightforward interpretation: it is simply the projection of the initial state on the degenerate subspace covered by $\hat{P}$. Its state vector is given by $\hat{P}|\psi_i\rangle = |\psi_{i'}\rangle$. Therefore, the argument of the weak value P_w is solely linked to the symplectic area of the geodesic triangle with vertices $|\psi_f\rangle$, $|\psi_i\rangle$ and $|\psi_{i'}\rangle$ and corresponds to the Pancharatnam–Berry phase (4). Indeed, the average value of a projector is always positive $\langle\psi_i|\hat{P}|\psi_i\rangle \geqslant 0$ and, thus, does not contribute to the geometric phase (16).

Another class of related observables gives rise to a nicely geometric interpretation of the projector $\hat{\Pi}_{i'}$ present in the effective Bargmann invariant. It comprises all the observables that are both unitary and Hermitian. Amongst them, we recover many multi-qubit quantum gates, such as the CNOT, CZ, SWAP, Toffoli and CSWAP gates, as well as, obviously, the Hadamard gate and all the Pauli gates acting on single qubits. Interestingly all the Hermitian unitary operators are connected to the projectors defined herebefore (28). Indeed from, any projector, we can build an observable $\hat{S} = 2\hat{P} - \hat{I}_N$ that is both Hermitian and unitary. Therefore,

$$\hat{S} = \frac{2k-N}{N}\hat{I}_N + \sqrt{\frac{2k(N-k)}{N}}\vec{\rho}\cdot\vec{L}, \tag{30}$$

where the unit vector $\vec{\rho}$ must obey the star product condition (29) since it is linked to a k-degenerate projector $\hat{P}$. The state produced by $(2\hat{P}-\hat{I}_N)|\psi_i\rangle = |\psi_{i'}\rangle$ results from a generalized reflection of the complex state vector $|\psi_i\rangle$ in $\mathbb{C}^N$ with respect to the subspace corresponding to $\hat{P}$. This provides us with a quite elegant interpretation of the state contributing to the effective Bargmann invariant, reminiscent of the role played by the mirror image of the initial vector on the Bloch sphere in the case of Pauli operators (see figure 2). For example, in qutrit systems, such an observable $\hat{S}$ would fundamentally flip the sign of one component of the state vector when it is expressed in the diagonal representation of the related projector $\hat{P}$. Therefore, the vector $\vec{i}'$ in S^7 would result from a peculiar reflection symmetry flipping the sign of the initial state vector components in four of the eight dimensions (in appendix E, see the expression (E.1) of an arbitrary state on S^7 given as a function of its Hilbert space representation, where one should change the sign of a component n_i). Additionally, since the observable is unitary, the geodesic arc connecting the states $|\psi_i\rangle$ and $|\psi_{i'}\rangle$ in $\mathbb{C}\mathrm{P}^{n-1}$ could correspond to an actual progressive evolution of the system.

8. Beyond weak measurements: average values and quantum uncertainties

Finally, we point out that we recover useful quantum mechanical expressions pertaining to average values of observables by setting identical initial and final states in the weak value (12). It is also helpful to look at expressions involving the variance in order to see how their definitions involve the star $\star$ and wedge $\wedge$ products of SU(N).

We suppose that the quantum system is in the state $|\psi\rangle$, characterized by the vector $\vec{i} = \vec{i}\star\vec{i}$. We consider two general observables $\hat{A} = a_I\hat{I}_N + a_L\,\vec{\alpha}\cdot\hat{\vec{L}}$ and $\hat{B} = b_I\hat{I}_N + b_L\,\vec{\beta}\cdot\hat{\vec{L}}$, where we use Greek letters for the operator vectors as they do not necessarily correspond to a state on the S^{N^2-2} sphere. Then the average value is related to the eight-dimensional Euclidean scalar product between the two vectors on the sphere:

$$\langle A\rangle = \langle\psi|\hat{A}|\psi\rangle = a_I + a_L\sqrt{2\frac{N-1}{N}}\,\vec{i}\cdot\vec{\alpha}, \tag{31}$$

where we set $\vec{f} = \vec{i}$ in (12). In appendix C, we compute the particular expressions of the squared operator $\hat{A}^2$, the commutator $[\hat{A},\hat{B}]$ and the anticommutator $\{\hat{A},\hat{B}\}$. These operators appear in the Heisenberg

uncertainty relations as

$$\mathrm{Var}(A)\,\mathrm{Var}(B) - \mathrm{Cov}^2(A,B) \geqslant \frac{1}{4}|\langle[\hat{A},\hat{B}]\rangle|^2, \tag{32}$$

where the variance is defined as usually by $\mathrm{Var}(A) = \langle A^2\rangle - \langle A\rangle^2$ and the (symmetric) covariance by $\mathrm{Cov}(A,B) = \frac{1}{2}\langle\{\hat{A},\hat{B}\}\rangle - \langle A\rangle\langle B\rangle$. Using these definitions, we find

$$\mathrm{Var}(A) = \frac{2}{N}a_L^2[1-(N-1)(\vec{\alpha}\cdot\vec{i})^2 + (N-2)\ \vec{\alpha}\star\vec{\alpha}\cdot\vec{i}] \tag{33}$$

$$\mathrm{Cov}(A,B) = \frac{2}{N}a_L b_L[\vec{\alpha}\cdot\vec{\beta} - (N-1)(\vec{\alpha}\cdot\vec{i})(\vec{\beta}\cdot\vec{i}) + (N-2)\ \vec{\alpha}\star\vec{\beta}\cdot\vec{i}] \tag{34}$$

$$\langle[\hat{A},\hat{B}]\rangle = 2\mathrm{i}a_L b_L\sqrt{2\frac{N-1}{N}}\ \vec{\alpha}\wedge\vec{\beta}\cdot\vec{i}. \tag{35}$$

Thus the two invariants that involve the wedge and star products that are present in the argument of weak values emerge as well in the Heisenberg uncertainty relationship. In particular, we observe that the numerator of the argument of the weak value, which involves the wedge product, is therefore proportional to an average, in the initial state, of a commutator. The operators in this commutator are the weakly measured observable and the final state. (Note that the roles of the initial and final state could be switched using a cyclic permutation of the three vectors.) Ultimately, these two invariants are built to provide contribution involving the three vectors in a fully symmetric or anti-symmetric way. It is suggested in the literature that the average value of the square of the commutator is a predictor of quantum chaos [86]. This can also be evaluated to be

$$\langle|[\hat{A},\hat{B}]|^2\rangle = \frac{8}{N}a_L b_L[\|\vec{\alpha}\wedge\vec{\beta}\|^2 + (N-2)(\vec{\alpha}\wedge\vec{\beta})\star(\vec{\alpha}\wedge\vec{\beta})\cdot\vec{i}]. \tag{36}$$

9. Conclusion

We described on hyperspheres the geometrical properties of the weak values of general observables. For projectors on pure states of N-level systems, the argument of the weak value is the argument the Bargmann invariant of the initial, projector and final states. The argument of the Bargmann invariant and, hence, the argument of the weak value represent a geometric phase that is associated to the symplectic area of the geodesic triangle in the projective space $\mathbb{C}\mathrm{P}^{N-1}$. The states are constrained to a $(2N-2)$-dimensional subspace of the unit sphere S^{N^2-2}, which generalizes the Bloch sphere. For all observables, we express the weak value and its argument in terms of three Euclidean vectors located on S^{N^2-2}: formulas involve the standard Euclidean scalar product, as well as two vectorial operations inherited from $\mathrm{SU}(N)$, represented by the star $\star$ and $\wedge$ products. We showed that the argument of the weak value is always related to a Bargmann invariant of three projectors, even when the observable probed by the weak measurement is not a projector. Thus we found a geometric depiction of the argument of any weak value in terms of a symplectic area of a geodesic triangle in complex projective space. For arbitrary observables of two-level systems, the geometric phase corresponds to minus half the solid angle subtended by the three vectors associated to the initial state, the effective projector linked to the weak value, and the final state. We studied on the Bloch sphere how the projector associated to the effective Bargmann invariant evolves as a function of the weakly probed observable in a two-level system. We also investigated the geometric operations behind this projector in higher dimensional systems, for arbitrary projectors on degenerate subspaces and for Hermitian quantum gates. We produced the weak values of the generators of $\mathrm{SU}(N)$, including the Pauli and Gell–Mann matrices, which are essential to all spin and polarization applications of weak measurements. The formalism used here applies to both weak and average values, and we illustrated its usefulness beyond weak measurements by expressing the quantities intervening in the Heisenberg inequalities.

We wish now to reflect on the significance of the argument of the weak value as a geometric phase. For the weak value of a projector $\hat{\Pi}_r$, we saw that this geometric phase is equivalent to the Pancharatnam–Berry phase that a state would acquire during a parametric evolution along the closed geodesic triangle formed by the initial state, the projector state and the final state. Actually, this corresponds also to the geometric phase for the open curve built from the two successive geodesics connecting $|\psi_i\rangle\langle\psi_i|$ to $|\psi_r\rangle\langle\psi_r|$, and then $|\psi_r\rangle\langle\psi_r|$ to $|\psi_f\rangle\langle\psi_f|$ [56]. Thus, we could be naively tempted to attribute this geometric phase to the final state after a post-selected weak-measurement of the projector $\hat{\Pi}_r$. However, our preliminary investigation of geometric phases during actual weak measurements shows that the geometric phase imparted on the joint system and Gaussian meter state, after post-selection but before meter measurement, does not depend on the weak coupling parameter g to first order (note that this geometric phase arises from a non-cyclic evolution, along

an open curve). Thus, the geometric phase acquired during a weak measurement with a Gaussian meter does not depend univocally on the associated weak value (to second order in the coupling parameter, it depends on the meter variance and on the imaginary part of weak value of the square of the observable: $\varphi_g \approx g^2\hbar^{-2}\Delta^2 p\,\Im\langle A^2\rangle_w$). Nevertheless, it is well-know [15] that, after a weak measurement with a Gaussian meter, the average meter position $\langle x\rangle$ is given by $g\,\Re A_w$, while the average meter momentum $\langle p\rangle$ is given by $2g\hbar^{-1}\Delta^2 p\,\Im A_w$. As a result, the argument of the weak value sets the angle pointing to the location of the centroid of the Gaussian Wigner function in the meter phase space after a weak measurement: $\arg A_w = \arctan\frac{\langle p\rangle\Delta x}{\langle x\rangle\Delta p}$ (this angle can be made equal to the geometric phase by an appropriate scaling of the phase space coordinates). Furthermore, Lundeen and Resch [87] showed that the weak value is proportional to the average α (in the final state $|\phi_m(fi)\rangle$ of the meter) of the annihilation operator $\hat{a}$ associated to the meter phase space. To first order in the coupling, after post-selection, the meter is thus left in a coherent state $|\alpha\rangle \approx |0\rangle + \alpha|1\rangle$ given by the eigenvalue $\alpha = g\hbar^{-1}\Delta p A_w$. Hence, the argument of the weak value appears as the phase of the coherent state, which is also the phase of its component in the first excited state $|1\rangle$. This approach provides as well a natural interpretation to the modulus of the weak value, as its square gives the average occupancy level in this coherent state: $\langle N\rangle_\alpha \approx g^2\hbar^{-2}\Delta^2 p|A_w|^2$.

In many weak measurements applications, we are actually interested in the meter shifted averages and not only in the operator weakly measured. For example, when measuring tiny optical deviations of light beams upon reflection on an interface (effects known as the Goos–Hänchen and Imbert–Fedorov shifts), the argument of the weak value would give an indication of the ratio of the observed angular to spatial shifts of the light beam. In such an experiment, the transverse position of the beam plays the role of the meter (subjected to shifts), while the weakly measured operator is an effective observable related to the transfer function of the reflection process (that depends on the polarization) [29]. The principle of performing a (typically amplified) weak measurement of an effective observable derived from the transfer function of a physical process is quite general [88]. Here, we provide some thoughts for the analysis of such ratios arising from experimental observations. The interpretation of the real and imaginary parts of the weak value have been much discussed in the literature. A useful point of view is that the real part of the weak value gives the optimal conditional estimate of the observable given the knowledge imparted by the initial and final states of the pre- and post-selected measurement [89–92]. Correspondingly, the imaginary part is related to the inaccuracy of the optimal estimate $\epsilon^2(\hat{F}) = \sum_f \Im^2 A_w(f)$, where f runs over all possible final states of the measurement observable $\hat{F}$ used for post-selection [89–92]. In some very broad sense, the ratio of the imaginary to the real part appears linked to the inverse of a signal-to-noise ratio. This observation can be made more precise by noting that the real part of the weak value has been linked in weak measurements to the role of the operator $\hat{A}$ as an observable, while the imaginary part has been associated to the operator $\hat{A}$ as the generator of infinitesimal unitary transformations $\mathrm{e}^{-\mathrm{i}\epsilon\hat{A}}$, where it plays a dynamical role [91, 93]. The argument of the weak value conveys thus a direct indication of the relative importance of these two aspects of the operator $\hat{A}$ in the physical process giving rise to the weak value. We further evidence this by expressing the weak value as a logarithmic derivative $A_w = \mathrm{i}\frac{\mathrm{d}}{\mathrm{d}\epsilon}\ln\langle\psi_f|\mathrm{e}^{-\mathrm{i}\epsilon\hat{A}}|\psi_i\rangle|_{\epsilon=0} = \mathrm{i}\frac{\mathrm{d}}{\mathrm{d}\epsilon}\ln\langle\psi_f|\psi(\epsilon)\rangle|_{\epsilon=0}$. By writing $\langle\psi_f|\psi(\epsilon)\rangle = R(\epsilon)\mathrm{e}^{\mathrm{i}S(\epsilon)}$ (with $R, S \in \mathbb{R}$), we find $A_w = -\frac{\mathrm{d}}{\mathrm{d}\epsilon}S(\epsilon) + \mathrm{i}\frac{\mathrm{d}}{\mathrm{d}\epsilon}\ln R(\epsilon)$. The argument of the weak value reflects then how the amplitude of the complex overlap between the final and initial states varies with respect to its phase in the limit of a vanishing evolution: $\arg A_w = -\frac{\mathrm{d}\ln R(\epsilon)}{\mathrm{d}S(\epsilon)}|_{\epsilon=0}$. We see that the derivative of the phase of the overlap encodes information about the observable (as the real part of the weak value corresponds to the best estimate), while the imaginary part of the weak value relates to the modification of the post-selection probability due to the unitary evolution through the logarithmic derivative of the overlap amplitude. The first aspect impacts the observed average meter position, while the second impacts its observed average momentum. As the argument is a geometric phase, we understand that the ratio of these very different aspects of the operator action in the weak value is fully determined by the geometry and can be represented and studied using geodesic triangles. This approach could be fruitful to study weak values arising from effective observables generated unitary transfer functions [88], and even could be generalized to non-Hermitian effective observables [29]. Although we were mainly concerned with discrete observables in this paper, it is nevertheless enlightening to review the former expressions in the context of the weak value of the momentum post-selected on position: $p_w = \mathrm{i}\hbar\frac{\mathrm{d}}{\mathrm{d}\epsilon}\ln\langle x|e^{-\frac{\mathrm{i}}{\hbar}\epsilon\hat{p}}|\psi_i\rangle|_{\epsilon=0} = \mathrm{i}\hbar\frac{\mathrm{d}}{\mathrm{d}\epsilon}\ln\psi(x-\epsilon)|_{\epsilon=0} = -\mathrm{i}\hbar\frac{\mathrm{d}}{\mathrm{d}x}\ln\psi(x)$, where now $R(x)$ and $S(x)$ are understood as the (real) amplitude and phase of the wavefunction $\psi(x)$ in the limit of an infinitesimal unitary transformation $e^{-\frac{\mathrm{i}}{\hbar}\epsilon\hat{p}}$. The argument provides thus the ratio of the so-called osmotic momentum $p_o = -\hbar\frac{\mathrm{d}}{\mathrm{d}x}\ln R(x) = \Im p_w$ and Bohmian momentum $p_b = \hbar\frac{\mathrm{d}}{\mathrm{d}x}S(x) = \Re p_w$ at position x [41, 90, 91]. The osmotic momentum p_o appears in the stochastic interpretation of quantum mechanics (with p_b), where it compensates the stochastic diffusion, while p_b is central in the de Broglie–Bohm interpretation as it defines deterministic particle velocities. The ratio of

these two momenta (or of the associated velocities) should thus be seen through the lens of geometric phases! The geometrical investigation of the argument of weak values advocates a holistic interpretation of the weak value as it describes the full observations in phase space, beyond the common dichotomy between the real and imaginary parts.

The geometric description applies to all weak values of discrete observables. Thus, it offers an extensive range of target applications. In particular, we believe our approach could prove useful to study the geometry of the connection between anomalous weak values and contextuality. Indeed, anomalous weak values are always a witness of contextuality [94, 95]. Additionally, anomalous weak values of arbitrary observables are necessarily linked to anomalous weak values of projectors [94, 95]. As the eigenvalue range of a projector is the [0, 1] interval, when the argument of a projector weak value is not equal to 0, the weak value is necessarily anomalous. Thus a non-zero argument of a projector weak value is an indicator of contextuality related to the emergence of a geometric phase. Furthermore, if the modulus of the weak value is larger than 1, this is also an indicator of contextuality. We could thus investigate from a geometrical viewpoint the nature of the contextuality that arise either from a non-zero argument or from an amplification effect. Beyond the projector case, any observable can be rescaled $(\hat{A} - \lambda_{\min}\hat{I})/(\lambda_{\max} - \lambda_{\min})$, so that its eigenvalue range belongs to the [0, 1] interval. Then, the argument and modulus of its weak values can be used similarly to the case of projectors to indicate contextuality.

Weak values also appear in dynamical processes [90], independently of weak measurements. For example, they determine the perturbed energy eigenvalues $E_n(g) = E_n(0) + \langle E_n(0)|\hat{\Delta}(g)|E_n(g)\rangle / \langle E_n(0)|E_n(g)\rangle$ due to a perturbation $\hat{\Delta}(g)$, in terms of the initial unperturbed energies $E_n(0)$ [90]. Thus, the positive or negative contributions of the different weak values for all the eigenstates could be analyzed from their argument (which control if the energies increase or decrease), by considering jointly the various geodesic triangles involved. Our formalism provides a description of the relevant weak values quantities in a geometric way in $\mathbb{R}^{N^2-1}$ that helps to visualize physical processes influenced by phases, in a conceptually simpler approach than in the complex Hilbert vector space. In this context, let us restate that a single weak value is determined by three states only. As a result, in any finite dimension, the geodesic triangle can be studied in a three dimensional subspace equivalent to $\mathbb{C}\mathrm{P}^2$. The geometric representation of a single weak value can thus be reduced to a qutrit case, which may simplify the geometric description (although not as much as in the qubit case). Focusing on qutrit systems is of prime importance to understand the geometry of weak values generally. In the example above, even if there are many energy eigenstates, for each of them, the problem reduces to a three dimensional subspace.

Finally, the appearance of geometric phases in weak values suggests that a geometric description of their argument should prove useful in fields in which the phase is essential, such as interferometry or quantum computing tasks. For example, beyond two-level systems, it would especially benefit to studies of the coupling of the three-dimensional polarization of light to its environment during propagation, of the orbital angular momentum of light beams used for quantum information processing tasks in large dimensions, of interferometers involving particles with spin larger than $\frac{1}{2}$, as well as of quantum paradoxes, where the phase plays an important role. Indeed, as we focused our attention to the argument of the weak value and its associated geometric phase, instead of the real part of the weak value (as is mostly done in the literature), we provide particular insight into the interferometric aspects of weak values and weak measurements.

Acknowledgments

YC is a Research Associate of the Fund for Scientific Research F.R.S.-FNRS. This research was supported by the Action de Recherche Concertée WeaM at the University of Namur (19/23-001).

Data availability statement

The data that support the findings of this study are available upon reasonable request from the authors.

Appendix A. Conventions for generators of SU(N)

In this paper, as a convention, we have chosen to use the $N^2 - 1$ traceless Hermitian generators of SU(N) that arise from the generalization of the Pauli and Gell–Mann matrices, thereafter noted $\hat{\vec{L}}$. From a strictly

formal point of view, these operators would probably be best seen as twice the proper generators of SU(N), typically noted $\hat{\vec{T}}$. However, we think this choice is natural in order to express quantum states on the Bloch sphere and generalized Bloch spheres in terms of standard operators. The generators usually defined by $\hat{\vec{T}}$ follow the properties

$$\left[\hat{T}_a, \hat{T}_b\right] = \mathrm{i}\sum_c f_{abc}\hat{T}_c, \tag{A.1}$$

$$\{\hat{T}_a, \hat{T}_b\} = \frac{1}{N}\delta_{ab}\hat{I}_N + \sum_c d_{abc}\hat{L}_c,$$

$$\mathrm{Tr}\ \hat{T}_a\hat{T}_b = \frac{1}{2}\delta_{ab},$$

$$\hat{T}_a\hat{T}_b = \frac{1}{2N}\delta_{ab}\hat{I}_N + \frac{1}{2}\sum_c \left(d_{abc} + \mathrm{i}f_{abc}\right)\hat{T}_c.$$

Even though these generators are mathematically convenient, quantum physics makes extensive use of the Pauli matrices $\hat{\vec{\sigma}}$. Their SU(3) counterparts are the well-known Gell–Mann matrices $\hat{\vec{\lambda}}$. They share the following properties with their SU(N) generalization $\hat{\vec{L}}$:

$$\left[\hat{L}_a, \hat{L}_b\right] = 2\mathrm{i}\sum_c f_{abc}\hat{L}_c, \tag{A.2}$$

$$\{\hat{L}_a, \hat{L}_b\} = \frac{4}{N}\delta_{ab}\hat{I}_N + 2\sum_c d_{abc}\hat{L}_c,$$

$$\mathrm{Tr}\ \hat{L}_a\hat{L}_b = 2\delta_{ab},$$

$$\hat{L}_a\hat{L}_b = \frac{2}{N}\delta_{ab}\hat{I}_N + \sum_c \left(d_{abc} + \mathrm{i}f_{abc}\right)\hat{L}_c.$$

The anti-symmetric structure constants and the symmetric constants of SU(N) are connected to the generators using

$$f_{abc} = -\frac{1}{4}\mathrm{i}\ \mathrm{Tr}(\hat{L}_a[\hat{L}_b, \hat{L}_c]) = -2\mathrm{i}\ \mathrm{Tr}(\hat{T}_a[\hat{T}_b, \hat{T}_c]), \tag{A.3}$$

$$d_{abc} = \frac{1}{4}\ \mathrm{Tr}(\hat{L}_a\{\hat{L}_b, \hat{L}_c\}) = 2\ \mathrm{Tr}(\hat{L}_a\{\hat{L}_b, \hat{L}_c\}), \tag{A.4}$$

so that $\hat{\vec{L}} = 2\,\hat{\vec{T}}$. This simple proportionality relationship provides the conversion rule between the two conventions, should anyone wish to use expressions with the $\hat{\vec{T}}$ generators. From now on, we will exclusively work with the $\hat{\vec{L}}$ generators.

Appendix B. Conventions for star product and projectors

From the symmetric constants d_{abc} of SU(N), we can construct a symmetric product called the star product. Given two (N^2-1)-dimensional vectors, the $\star$ product produces a vector with components $(\vec{\alpha}\star\vec{\beta})_c = c_s\sum_{ab} d_{abc}\alpha_a\beta_b$, where c_s is a proportionality constant. It would be convenient to simply set $c_s = 1$ (as done for the definition of the anti-symmetric wedge product $(\vec{\alpha}\wedge\vec{\beta})_c = \sum_{ab} f_{abc}\alpha_a\beta_b$, which is built on the structure constants). However, the original definition of the star product in the literature [77, 78] used another convention: the star product identified a proper quantum state from $\mathbb{C}P^2$ on the S^7 sphere. In the following, we explain thus how we generalized the star product from SU(3) to SU(N), based on this earlier choice. We also explain our normalization convention for projectors, as they are related.

A general projector $\hat{P}$ in $\mathbb{C}^N\times\mathbb{C}^N$ acting on states in $\mathbb{C}^N$ is defined by the relation $\hat{P}^2 = \hat{P}$. In addition, its trace is an integer number that is lower or equal to the dimension N: $\mathrm{Tr}\ \hat{P} = k$, with $1\leqslant k\leqslant N$ representing the dimension of the projector subspace (essentially the degeneracy of the eigenvalue 1). We pose $\hat{P} = \frac{k}{N}\hat{I}_N + c_p\,\vec{\beta}\cdot\hat{\vec{L}}$ to meet the trace condition. The positive constant

$$c_p = \sqrt{\frac{k(N-k)}{2N}} \tag{B.1}$$

ensures that $\vec{\beta}$ is always a normalized vector ($\vec{\beta}\cdot\vec{\beta}=1$) on the S^{N^2-2} unit sphere. Its value originates from the projector condition

$$\hat{P}^2=\left(\frac{k^2}{N^2}+\frac{2}{N}c_p^2\right)\hat{I}_N+\frac{2k}{N}c_p\ \vec{\beta}\cdot\hat{\vec{L}}+c_p^2\sum_{abc}d_{abc}\beta_a\beta_b\hat{L}_c=\frac{k}{N}\hat{I}_N+c_p\,\vec{\beta}\cdot\hat{\vec{L}}, \tag{B.2}$$

where we used (A.2) to expand the SU(N) generator square $(\vec{n}\cdot\hat{\vec{L}})^2$. Additionally, (B.2) constraints the vector $\vec{\beta}$ through the star product

$$\frac{1}{c_s}(\vec{\beta}\star\vec{\beta})_c=\sum_{ab}d_{abc}\beta_a\beta_b=\left(1-\frac{2k}{N}\right)\frac{1}{c_p}\beta_c. \tag{B.3}$$

In the literature [77, 78], the star product was defined in SU(3) by imposing that this condition becomes $\vec{\beta}\star\vec{\beta}=\vec{\beta}$ for projectors on pure states (case $k=1$). Therefore, imposing $\vec{\beta}\star\vec{\beta}=\vec{\beta}$ for pure states, we find the value of the constant c_s in SU(N):

$$c_s=\frac{Nc_p}{N-2}=\frac{1}{N-2}\sqrt{\frac{N(N-1)}{2}}, \tag{B.4}$$

which thus defines the star product in SU(N) [81]. As a result, an arbitrary projector takes the form

$$\hat{P}=\frac{k}{N}\hat{I}_N+\sqrt{\frac{k(N-k)}{2N}}\,\vec{\beta}\cdot\hat{\vec{L}}, \tag{B.5}$$

with the accompanying star product constraint resulting from (B.3):

$$\vec{\beta}\star\vec{\beta}=\frac{N-2k}{N-2}\sqrt{\frac{N-1}{k(N-k)}}\vec{\beta}. \tag{B.6}$$

Note that, only when $k=1$, does this projector correspond to a quantum state from $\mathbb{C}\mathrm{P}^{n-1}$. For example, a projector on an $(N-1)$-dimensional subspace obeys $\vec{\beta}\star\vec{\beta}=-\vec{\beta}$; it is the opposite of the vector associated to the projection on the complementary one-dimensional subspace (this one is a quantum state).

In summary, our convention sets the constant c_p defining an arbitrary projector so that we always work with vectors belonging to hyperspheres of unit radius when using the operators $\hat{\vec{L}}$ as generators of SU(N) [71, 77–79, 81]. Then, in order to define the star product, we follow the literature convention that the set of vectors representing pure quantum states is equivalent to the vectors invariant under the star product (in the sense of $\vec{r}\star\vec{r}=\vec{r}$) [71, 77–79, 81]. We note that, when working with generalized Bloch spheres, some authors prefer to set $c_p=1$ and deal with unnormalized vectors [69, 70]. This would be inconvenient for us, as many expressions linked to weak values are invariant under permutations of the related vectors, some of which would be normalized and others not. Managing the vector normalization status complicates geometric descriptions as well. On the other hand, if the star product were defined initially with the constant $c_s=1$, the constant c_s would not appear when the product of two generators is expressed in terms of the star product, such as in the weak value formula (C.13). Were it the case, the projector condition for pure state would have been $\vec{r}\star\vec{r}=\frac{1}{c_s}\vec{r}$. A few authors working with unnormalized vectors chose to redefine to the star product with $c_s=1$ [80, 82].

Appendix C. Computation of the weak value and Bargmann invariant

Computing weak values involves the traces of products of two and three operators. Considering three arbitrary generators $\vec{\alpha}\cdot\hat{\vec{L}}$, $\vec{\beta}\cdot\hat{\vec{L}}$ and $\vec{\gamma}\cdot\hat{\vec{L}}$, using (A.2), we find the products and traces

$$(\vec{\alpha}\cdot\hat{\vec{L}})(\vec{\beta}\cdot\hat{\vec{L}})=\frac{2}{N}\vec{\alpha}\cdot\vec{\beta}\ \hat{I}_N+\frac{1}{c_s}(\vec{\alpha}\star\vec{\beta})\cdot\hat{\vec{L}}+\mathrm{i}\ (\vec{\alpha}\wedge\vec{\beta})\cdot\hat{\vec{L}}, \tag{C.1}$$

$$\mathrm{Tr}[(\vec{\alpha}\cdot\hat{\vec{L}})(\vec{\beta}\cdot\hat{\vec{L}})]=2\ \vec{\alpha}\cdot\vec{\beta}, \tag{C.2}$$

where c_s is defined in (B.4). For three generators, we have

$$(\vec{\alpha}\cdot\hat{\vec{L}})(\vec{\beta}\cdot\hat{\vec{L}})(\vec{\gamma}\cdot\hat{\vec{L}})=\frac{2}{N}\left[\frac{1}{c_s}(\vec{\alpha}\star\vec{\beta})\cdot\vec{\gamma}+\mathrm{i}(\vec{\alpha}\wedge\vec{\beta})\cdot\vec{\gamma}\right]\hat{I}_N$$
$$+\frac{2}{N}\vec{\alpha}\cdot\vec{\beta}\ (\vec{\gamma}\cdot\hat{\vec{L}})+\frac{1}{c_s^2}[(\vec{\alpha}\star\vec{\beta})\star\vec{\gamma}]\cdot\hat{\vec{L}}-\ [(\vec{\alpha}\wedge\vec{\beta})\wedge\vec{\gamma}]\cdot\hat{\vec{L}}$$

$$+\,\mathrm{i}\frac{1}{c_s}\Big\{[(\vec{\alpha}\wedge\vec{\beta})\star\vec{\gamma}]\cdot\hat{\vec{L}}+[(\vec{\alpha}\star\vec{\beta})\wedge\vec{\gamma}]\cdot\hat{\vec{L}}\Big\}, \tag{C.3}$$

$$\mathrm{Tr}[(\vec{\alpha}\cdot\hat{\vec{L}})(\vec{\beta}\cdot\hat{\vec{L}})(\vec{\gamma}\cdot\hat{\vec{L}})]=\frac{2}{c_s}(\vec{\alpha}\star\vec{\beta})\cdot\vec{\gamma}+2\mathrm{i}\;(\vec{\alpha}\wedge\vec{\beta})\cdot\vec{\gamma}. \tag{C.4}$$

As the trace is invariant under unitary transformations, we see that the two quantities $(\vec{\alpha}\star\vec{\beta})\cdot\vec{\gamma}$ and $(\vec{\alpha}\wedge\vec{\beta})\cdot\vec{\gamma}$ present in (C.4) are also invariant under unitary transformations. From the properties of the d_{abc} and f_{abc} constants of SU(N), the former is fully symmetric under permutations, while the latter is antisymmetric and changes sign under permutation of two vectors.

Now we define two projectors on pure states $\hat{\Pi}_i=\frac{1}{N}\hat{I}_N+c_p\;\vec{i}\cdot\hat{\vec{L}}$ and $\hat{\Pi}_f=\frac{1}{N}\hat{I}_N+c_p\;\vec{f}\cdot\hat{\vec{L}}$ (with c_p given by (B.1) with $k=1$), as well as two arbitrary Hermitian operators $\hat{A}=a_I\hat{I}_N+a_L\;\vec{\alpha}\cdot\hat{\vec{L}}$ and $\hat{B}=b_I\hat{I}_N+b_L\;\vec{\beta}\cdot\hat{\vec{L}}$. Following (C.1), the product of the operators $\hat{A}$ and $\hat{B}$ becomes

$$\begin{aligned}\hat{A}\hat{B}&=a_Ib_I\hat{I}_N+a_Lb_I\;\vec{\alpha}\cdot\hat{\vec{L}}+a_Ib_L\;\vec{\beta}\cdot\hat{\vec{L}}+a_Lb_L(\vec{\alpha}\cdot\hat{\vec{L}})(\vec{\beta}\cdot\hat{\vec{L}})\\&=\left(a_Ib_I+\frac{2}{N}a_Lb_L\;\vec{\alpha}\cdot\vec{\beta}\right)\hat{I}_N+a_Lb_I\;\vec{\alpha}\cdot\hat{\vec{L}}+a_Ib_L\;\vec{\beta}\cdot\hat{\vec{L}}+a_Lb_L\frac{1}{c_s}\;(\vec{\alpha}\star\vec{\beta})\cdot\hat{\vec{L}}+\mathrm{i}a_Lb_L\;(\vec{\alpha}\wedge\vec{\beta})\cdot\hat{\vec{L}}.\end{aligned} \tag{C.5}$$

When $\hat{A}=\hat{B}$, the latter simplifies to

$$\hat{A}^2=\left(a_I^2+\frac{2}{N}a_L^2\right)\hat{I}_N+2a_Ia_L\;\vec{\alpha}\cdot\hat{\vec{L}}+a_L^2\frac{1}{c_s}\;(\vec{\alpha}\star\vec{\alpha})\cdot\hat{\vec{L}}. \tag{C.6}$$

These expressions also allow us to compute the commutator and anti-commutator

$$[\hat{A},\hat{B}]=2\mathrm{i}a_Lb_L\;(\vec{\alpha}\wedge\vec{\beta})\cdot\hat{\vec{L}} \tag{C.7}$$

$$\{\hat{A},\hat{B}\}=2\left(a_Ib_I+\frac{2}{N}a_Lb_L\;\vec{\alpha}\cdot\vec{\beta}\right)\hat{I}_N+2a_Lb_I\;\vec{\alpha}\cdot\hat{\vec{L}}+2a_Ib_L\;\vec{\beta}\cdot\hat{\vec{L}}+2a_Lb_L\frac{1}{c_s}\;(\vec{\alpha}\star\vec{\beta})\cdot\hat{\vec{L}}. \tag{C.8}$$

The latter were used in section 8 to compute the variance and covariance of operators. Formula (C.5) gives the product $\hat{\Pi}_f\hat{\Pi}_i$ of the two projectors, by simply setting $a_I=b_I=\frac{1}{N}$ and $a_L=b_L=c_p$, so that the trace of two projectors is

$$\mathrm{Tr}\,(\hat{\Pi}_f\hat{\Pi}_i)=\frac{1}{N}+2c_p^2\;\vec{f}\cdot\vec{i}=\frac{1}{N}[1+(N-1)\;\vec{f}\cdot\vec{i}\,]. \tag{C.9}$$

This is the denominator of the weak value (1). To obtain its numerator, we evaluate

$$\begin{aligned}\hat{\Pi}_f\hat{A}\hat{\Pi}_i=&\frac{a_I}{N^2}\hat{I}_N+\frac{a_I}{N}c_p\;\vec{i}\cdot\hat{\vec{L}}+\frac{a_L}{N^2}\;\vec{\alpha}\cdot\hat{\vec{L}}+\frac{a_L}{N}c_p(\vec{\alpha}\cdot\hat{\vec{L}})(\vec{i}\cdot\hat{\vec{L}})\\&+\frac{a_I}{N}c_p\;\vec{f}\cdot\hat{\vec{L}}+a_Ic_p^2(\vec{f}\cdot\hat{\vec{L}})(\vec{i}\cdot\hat{\vec{L}})+\frac{a_L}{N}c_p(\vec{f}\cdot\hat{\vec{L}})(\vec{\alpha}\cdot\hat{\vec{L}})+a_Lc_p^2(\vec{f}\cdot\hat{\vec{L}})(\vec{\alpha}\cdot\hat{\vec{L}})(\vec{i}\cdot\hat{\vec{L}}).\end{aligned} \tag{C.10}$$

Then, the trace formulas (C.2) and (C.4) yield

$$\mathrm{Tr}\,(\hat{\Pi}_f\hat{A}\hat{\Pi}_i)=\frac{a_I}{N}+2\frac{a_L}{N}c_p\;\vec{\alpha}\cdot\vec{i}+2a_Ic_p^2\;\vec{f}\cdot\vec{i}+2\frac{a_L}{N}c_p\;\vec{f}\cdot\vec{\alpha}+2a_Lc_p^2\left[\frac{1}{c_s}(\vec{f}\star\vec{\alpha})\cdot\vec{i}+\mathrm{i}\;(\vec{f}\wedge\vec{\alpha})\cdot\vec{i}\right]. \tag{C.11}$$

The Bargmann invariant ensues from considering that $\hat{A}=\hat{\Pi}_r$ ($a_I=\frac{1}{N}$ and $a_L=c_p$),

$$\mathrm{Tr}\,(\hat{\Pi}_f\hat{\Pi}_r\hat{\Pi}_i)=\frac{1}{N^2}+\frac{2}{N}c_p^2(\vec{r}\cdot\vec{i}+\vec{f}\cdot\vec{i}+\vec{f}\cdot\vec{r})+2c_p^3\left[\frac{1}{c_s}(\vec{f}\star\vec{r})\cdot\vec{i}+\mathrm{i}\;(\vec{f}\wedge\vec{r})\cdot\vec{i}\right], \tag{C.12}$$

while the weak value is simply given by the ratio of (C.11) with (C.9). The real and imaginary part of the weak value are thus

$$\Re\,A_w=\frac{\frac{a_I}{N}+\frac{2a_L}{N}c_p(\vec{\alpha}\cdot\vec{i}+\vec{f}\cdot\vec{\alpha})+2a_Ic_p^2\;\vec{f}\cdot\vec{i}+2a_Lc_p^2\frac{1}{c_s}(\vec{f}\star\vec{\alpha})\cdot\vec{i}}{\frac{1}{N}+2c_p^2\;\vec{f}\cdot\vec{i}}, \tag{C.13}$$

$$\Im\,A_w=\frac{2\mathrm{i}\,a_Lc_p^2\;(\vec{f}\wedge\vec{\alpha})\cdot\vec{i}}{\frac{1}{N}+2c_p^2\;\vec{f}\cdot\vec{i}}. \tag{C.14}$$

The argument of the weak value is determined by $\arctan(\Im\,A_w/\Re\,A_w)$ while simultaneously taking the signs of (C.13) and (C.14) into account to recover the appropriate quadrant. The latter expressions allow for an

easy conversion between possibly different conventions for the c_p and c_s constants, as discussed in appendix B.

Appendix D. Properties of states on S^{N^2-2} and the $\star$ and $\wedge$ products

In this section, we review a few properties of the state representation on the generalized Bloch sphere, in connection to the $\star$ and $\wedge$ products of SU(N), as we believe this formalism is still unfamiliar to many. Our goal is to provide a glimpse on key aspects of the geometry and highlight information relevant to interpreting the various contributions to weak value formulas.

First of all, we consider the conditions defining an orthonormal basis of $\mathbb{C}\mathrm{P}^{n-1}$: the projector orthogonality relationship $\hat{\vec{\Pi}}_i\hat{\vec{\Pi}}_j = \delta_{ij}\hat{\vec{\Pi}}_i$, as well as the resolution of the identity $\sum_{i=1}^{N}\hat{\Pi}_i = \hat{I}_N$. For orthogonal states, the former impose that the angles between the vectors are given by $\vec{n}_i \cdot \vec{n}_j = -\frac{1}{N-1}$ (C.9). In addition, the later results in $\sum_i \vec{n}_i = 0$. Thus, the vectors are all placed very symmetrically. For SU(2), these conditions show that vectors associated to orthogonal states are opposite, a well-known property of the standard Bloch sphere. For SU(3), the three vectors arising from a state basis all lie in a plane, with angles of 120° between them: their extremities form an equilateral triangle. For SU(4), the vectors build a tetrahedron. In larger dimensions, for SU(N), the arrangements remain extremely symmetric in a similar fashion, with the N vectors residing in a subspace of $N-1$ dimensions. We see thus that orthogonal states do not correspond to orthogonal vectors in the Euclidean sense. Actually, an orthogonal vector $\vec{r}$ verifying $\vec{r}\cdot\vec{n}_i = 0$ for all states of a given basis, obeys $\mathrm{Tr}\,(\hat{\Pi}_r\hat{\Pi}_i) = \frac{1}{N}$ (C.9). It corresponds to a state with maximal relative uncertainty with respect to the measurement basis (such as between states belonging to two different mutually unbiased bases). Orthogonal quantum states verify the following two additional relationships for their associated vectors: their wedge product is null $\vec{m}\wedge\vec{n} = 0$ and their star product is located on the angle bissector of the two vectors $\vec{m}\star\vec{n} = -\frac{1}{N-2}(\vec{m}+\vec{n})$. In the particular case of SU(3), the later results in the third basis vector being given by the star product of the other two ($\vec{n}_1\star\vec{n}_2 = \vec{n}_3$).

The symmetric star product is not associative. The star product of an arbitrary normalized vector $\vec{\alpha}$ does not generally produce a normalized vector ($\|\vec{\alpha}\star\vec{\alpha}\| \neq 1$), with the exception of SU(3), where $\vec{\alpha}\star\vec{\alpha}$ always remains on S^7. Of course, all vectors associated to pure states also remain on S^{N^2-2} in this manner, following the choice set by the definition of the $\star$ product. As the star product defines the condition for a vector to represent a state ($\vec{r}\star\vec{r} = \vec{r}$), we consider the particular case of the star product between two vectors associated to states. In that particular case, we have $(\vec{q}\star\vec{r})\cdot\vec{q} = (\vec{q}\star\vec{r})\cdot\vec{r} = \vec{q}\cdot\vec{r}$ (thanks to the fully symmetric nature of the product). Therefore, the star product of two projectors lies in the median hyperplane lying between $\vec{q}$ and $\vec{r}$, which is orthogonal to $\vec{q}-\vec{r}$, as could be expected from the symmetric properties of the product. In general, the star product of two vectors $\vec{q}$, $\vec{r}$ does not remain in the plane spanned by the two vectors (contrary to what we observed for two orthogonal states). Neither does it represent a state in general. We note that, operationally, an observable involving the vector $\vec{\alpha}\star\vec{\alpha}$ can be constructed from the square of an operator $(\vec{\alpha}\cdot\hat{\vec{L}})^2 = \frac{2}{N}\hat{I}_N + \frac{1}{c_s}[(\vec{\alpha}\star\vec{\alpha})\cdot\hat{\vec{L}}]$ (C.6), so that this vector contributes to quantum fluctuations (see section 8).

The anti-symmetric wedge product is not associative. It produces a vector orthogonal to the initial ones: $\vec{\alpha}\wedge\vec{\alpha} = 0$ and, therefore, $\vec{\alpha}\wedge\vec{\beta}\cdot\vec{\alpha} = \vec{\alpha}\wedge\vec{\beta}\cdot\vec{\beta} = 0$. However, due to the large number of dimensions involved, the wedge product selects an orthogonal direction amongst many available (contrary to the cross-product in three dimensions, for which the orthogonal direction to two non-parallel vectors is unique). The wedge product is intimately associated to the commutator (C.7). From the Baker–Campbell–Hausdorff formula, the wedge product gives the unitary operator associated to the non-commutativity of consecutive unitary transformations, such as the generators of rotations: $e^{-\mathrm{i}g\vec{\beta}\cdot\hat{\vec{L}}}e^{-\mathrm{i}g\vec{\alpha}\cdot\hat{\vec{L}}}e^{\mathrm{i}g\vec{\beta}\cdot\hat{\vec{L}}}e^{\mathrm{i}g\vec{\alpha}\cdot\hat{\vec{L}}} \approx e^{\mathrm{i}g^2(\vec{\alpha}\wedge\vec{\beta})\cdot\hat{\vec{L}}}$. From a practical point of view, this allows to construct an observable linked to the wedge product. This product gives thus also the direction of the effective transformation of an observable undergoing a small unitary transformation (from (C.7) as $e^{\mathrm{i}g\hat{A}}\hat{B}e^{-\mathrm{i}g\hat{A}} \approx \hat{B} + \mathrm{i}g[\hat{A},\hat{B}]$).

The wedge and star products between two vectors representing states are orthogonal in the following sense: $(\vec{q}\star\vec{r})\cdot(\vec{q}\wedge\vec{r}) = 0$ (actually, we also checked up to SU(6) using brute force calculation with a computer algebra system that this is true for any two vectors). Other relationships connect the star an wedge products in the case of pure states. By imposing that a projector $\hat{\Pi}_r$ remains a projector after a unitary transformation with generator $\vec{\alpha}\cdot\hat{\vec{L}}$, to first order, we obtain $\vec{\alpha}\wedge\vec{r} = 2\vec{r}\star(\vec{\alpha}\wedge\vec{r})$ (and more complex relationships can be deduced from second-order contributions).

Appendix E. $\mathbb{C}P^2$ representation on S^7

Considering an arbitrary state $|\psi\rangle$, the coordinates on the corresponding hypersphere are obtained by $\mathrm{Tr}\,\hat{\Pi}_\psi\hat{\tilde{L}}$. On S^7, the state $|\psi\rangle = \left(n_1 e^{i\chi_1}, n_2 e^{i\chi_2}, n_3 e^{i\chi_3}\right)^{\mathrm{T}}$ would thus become the gauge-invariant vector

$$\Big[n_1 n_2\,\cos(\chi_1-\chi_2), -n_1 n_2\,\sin(\chi_1-\chi_2), \frac{1}{2}(n_1^2-n_2^2), n_1 n_3\,\cos(\chi_1-\chi_3),$$
$$-n_1 n_3\,\sin(\chi_1-\chi_3), n_2 n_3\,\cos(\chi_2-\chi_3), -n_2 n_3\,\sin(\chi_2-\chi_3), \frac{1}{2\sqrt{3}}(n_1^2+n_2^2-2n_3^2)\Big]^{\mathrm{T}}. \tag{E.1}$$

A closed geodesic $(0,\ \sin s, \cos s)^{\mathrm{T}}$ $(s\in[0,\pi])$ appears therefore as a tilted circle of radius $\sqrt{3}/2$ on S^7 (it is not a great-circle):

$$\Big[0,0,-\frac{\sqrt{3}}{4}(1-\cos\,2s),0,0,\frac{\sqrt{3}}{2}\,\sin\,2s,0,-\frac{1}{4}(1+3\,\cos\,2s)\Big]^{\mathrm{T}}. \tag{E.2}$$

ORCID iDs

Lorena Ballesteros Ferraz https://orcid.org/0000-0003-3755-0201
Dominique L Lambert https://orcid.org/0000-0002-6415-3175
Yves Caudano https://orcid.org/0000-0002-0805-4068

References

[1] Acín A *et al* 2018 The quantum technologies roadmap: a European community view *New J. Phys.* **20** 080201
[2] Laucht A *et al* 2021 Roadmap on quantum nanotechnologies *Nanotechnology* **32** 162003
[3] Deutsch I H 2020 Harnessing the power of the second quantum revolution *PRX Quantum* **1** 020101
[4] Leontica S, Tennie F and Farrow T 2021 Simulating molecules on a cloud-based five-qubit IBM-Q universal quantum computer *Commun. Phys.* **4** 112
[5] Bian K, Zheng W, Zeng X, Chen X, Stöhr R, Denisenko A, Yang S, Wrachtrup J and Jiang Y 2021 Nanoscale electric-field imaging based on a quantum sensor and its charge-state control under ambient condition *Nat. Commun.* **12** 2457
[6] Cooke A-K, Champollion C and Le Moigne N 2021 First evaluation of an absolute quantum gravimeter (AQG#B01) for future field experiments *Geosci. Instrum. Method Data Syst.* **10** 65–79
[7] Busch P, Lahti P, Pellonpää J P and Ylinen K 2016 *Quantum Measurement Theoretical and Mathematical Physics* (Berlin: Springer)
[8] Jacobs K 2014 *Quantum Measurement Theory and its Applications* (Cambridge: Cambridge University Press)
[9] Mello P A 2014 The von Neumann model of measurement in quantum mechanics *AIP Conf. Proc.* **1575** 136–65
[10] Fuchs C A and Peres A 1996 Quantum-state disturbance versus information gain: uncertainty relations for quantum information *Phys. Rev.* A **53** 2038–45
[11] Naus H W L 2021 On the quantum mechanical measurement process *Found. Phys.* **51** 1–13
[12] Aharonov Y, Albert D Z and Vaidman L 1988 How the result of a measurement of a component of the spin of a spin-1/2 particle can turn out to be 100 *Phys. Rev. Lett.* **60** 1351
[13] Svensson B E Y 2013 Pedagogical review of quantum measurement theory with an emphasis on weak measurements *Quanta* **2** 18–49
[14] Dressel J, Malik M, Miatto F M, Jordan A N and Boyd R W 2014 Colloquium: understanding quantum weak values: basics and applications *Rev. Mod. Phys.* **86** 307–16
[15] Jozsa R 2007 Complex weak values in quantum measurement *Phys. Rev.* A **76** 044103
[16] Zhang L, Datta A and Walmsley I A 2015 Precision metrology using weak measurements *Phys. Rev. Lett.* **114** 210801
[17] Xu L, Liu Z, Datta A, Knee G C, Lundeen J S, Lu Y Q and Zhang L 2020 Approaching quantum-limited metrology with imperfect detectors by using weak-value amplification *Phys. Rev. Lett.* **125** 080501
[18] Xu X Y, Kedem Y, Sun K, Vaidman L, Li C F and Guo G C 2013 Phase estimation with weak measurement using a white light source *Phys. Rev. Lett.* **111** 033604
[19] Hallaji M, Feizpour A, Dmochowski G, Sinclair J and Steinberg A M 2017 Weak-value amplification of the nonlinear effect of a single photon *Nat. Phys.* **13** 540–4
[20] Qiu X, Xie L, Liu X, Luo L, Zhang Z and Du J 2016 Estimation of optical rotation of chiral molecules with weak measurements *Opt. Lett.* **41** 4032–5
[21] Li D, Shen Z, He Y, Zhang Y, Chen Z and Ma H 2016 Application of quantum weak measurement for glucose concentration detection *Appl. Opt.* **55** 1697–702
[22] Li D, Guan T, He Y, Liu F, Yang A, He Q, Shen Z and Xin M 2018 A chiral sensor based on weak measurement for the determination of Proline enantiomers in diverse measuring circumstances *Biosens. Bioelectron.* **110** 103–9
[23] Dixon P B, Starling D J, Jordan A N and Howell J C 2009 Ultrasensitive beam deflection measurement via interferometric weak value amplification *Phys. Rev. Lett.* **102** 173601
[24] Magaña-Loaiza O S, Mirhosseini M, Rodenburg B and Boyd R W 2014 Amplification of angular rotations using weak measurements *Phys. Rev. Lett.* **112** 200401
[25] Harris J, Boyd R W and Lundeen J S 2017 Weak value amplification can outperform conventional measurement in the presence of detector saturation *Phys. Rev. Lett.* **118** 070802

[26] Jordan A N, Martínez-Rincón J and Howell J C 2014 Technical advantages for weak-value amplification: when less is more *Phys. Rev.* X **4** 011031
[27] Hosten O and Kwiat P 2008 Observation of the spin Hall effect of light via weak measurements *Science* **319** 787–90
[28] Jayaswal G, Mistura G and Merano M 2013 Weak measurement of the Goos–Hänchen shift *Opt. Lett.* **38** 1232–4
[29] Dennis M R and Götte J B 2012 The analogy between optical beam shifts and quantum weak measurements *New J. Phys.* **14** 073013
[30] Ling X, Zhou X, Huang K, Liu Y, Qiu C-W, Luo H and Wen S 2017 Recent advances in the spin Hall effect of light *Rep. Prog. Phys.* **80** 066401
[31] Lundeen J S, Sutherland B, Patel A, Stewart C and Bamber C 2011 Direct measurement of the quantum wavefunction *Nature* **474** 188–91
[32] Malik M, Mirhosseini M, Lavery M P J, Leach J, Padgett M J and Boyd R W 2014 Direct measurement of a 27-dimensional orbital-angular-momentum state vector *Nat. Commun.* **5** 3115
[33] Wu S 2013 State tomography via weak measurements *Sci. Rep.* **3** 1193
[34] Goggin M E, Almeida M P, Barbieri M, Lanyon B P, O'Brien J L, White A G and Pryde G J 2011 Violation of the Leggett–Garg inequality with weak measurements of photons *Proc. Natl Acad. Sci. USA* **108** 1256–61
[35] Rozema L A, Darabi A, Mahler D H, Hayat A, Soudagar Y and Steinberg A M 2012 Violation of Heisenberg's measurement-disturbance relationship by weak measurements *Phys. Rev. Lett.* **109** 100404
[36] Matzkin A 2019 Weak values and quantum properties *Found. Phys.* **49** 298–316
[37] Resch K J, Lundeen J S and Steinberg A M 2004 Experimental realization of the quantum box problem *Phys. Lett.* A **324** 125–31
[38] Yokota K, Yamamoto T, Koashi M and Imoto N 2009 Direct observation of Hardy's paradox by joint weak measurement with an entangled photon pair *New J. Phys.* **11** 033011
[39] Denkmayr T, Geppert H, Sponar S, Lemmel H, Matzkin A, Tollaksen J and Hasegawa Y 2014 Observation of a quantum Cheshire cat in a matter-wave interferometer experiment *Nat. Commun.* **5** 4492
[40] Chen M-C *et al* 2019 Experimental demonstration of quantum pigeonhole paradox *Proc. Natl Acad. Sci. USA* **116** 1549–52
[41] Kocsis S, Braverman B, Ravets S, Stevens M J, Mirin R P, Shalm L K and Steinberg A M 2011 Observing the average trajectories of single photons in a two-slit interferometer *Science* **332** 1170–3
[42] Bliokh K Y, Bekshaev A Y, Kofman A G and Nori F 2013 Photon trajectories, anomalous velocities and weak measurements: a classical interpretation *New J. Phys.* **15** 073022
[43] Matzkin A 2012 Observing trajectories with weak measurements in quantum systems in the semiclassical regime *Phys. Rev. Lett.* **109** 150407
[44] Lund A P 2011 Efficient quantum computing with weak measurements *New J. Phys.* **13** 053024
[45] Martínez-Rincón J 2017 Overcoming experimental limitations in a nonlinear two-qubit gate through postselection *Quantum Inf. Process.* **16** 45
[46] Singh U and Pati A K 2014 Quantum discord with weak measurements *Ann. Phys., NY* **343** 141–52
[47] Gross J A, Caves C M, Milburn G J and Combes J 2018 Qubit models of weak continuous measurements: Markovian conditional and open-system dynamics *Quantum Sci. Technol.* **3** 024005
[48] Weber S J, Chantasri A, Dressel J, Jordan A N, Murch K W and Siddiqi I 2014 Mapping the optimal route between two quantum states *Nature* **511** 570–3
[49] Brun T A, Diósi L and Strunz W T 2008 Test of weak measurement on a two- or three-qubit computer *Phys. Rev.* A **77** 032101
[50] Kato T 1950 On the adiabatic theorem of quantum mechanics *J. Phys. Soc. Japan* **5** 435–9
[51] Pancharatnam S 1956 Generalized theory of interference, and its applications *Proc. Indian Acad. Sci.* **44** 247–62
[52] Longuet-Higgins H C, Öpik U, Pryce M H L and Sack R 1958 Studies of the Jahn–Teller effect: II. The dynamical problem *Proc. R. Soc.* A **244** 1–16
[53] Berry M V 1984 Quantal phase factors accompanying adiabatic changes *Proc. R. Soc.* A **392** 45–57
[54] Shapere A and Wilczek F 1989 *Geometric Phases in Physics* vol 5 (Singapore: World Scientific)
[55] Aharonov Y and Anandan J 1987 Phase change during a cyclic quantum evolution *Phys. Rev. Lett.* **58** 1593–6
[56] Mukunda N and Simon R 1993 Quantum kinematic approach to the geometric phase: I. General formalism *Ann. Phys., NY* **228** 205–68
[57] Cohen E, Larocque H, Bouchard F, Nejadsattari F, Gefen Y and Karimi E 2019 Geometric phase from Aharonov–Bohm to Pancharatnam–Berry and beyond *Nat. Rev. Phys.* **1** 437–49
[58] Sjöqvist E 2006 Geometric phase in weak measurements *Phys. Lett.* A **359** 187–9
[59] Tamate S, Kobayashi H, Nakanishi T, Sugiyama K and Kitano M 2009 Geometrical aspects of weak measurements and quantum erasers *New J. Phys.* **11** 093025
[60] Kedem Y and Vaidman L 2010 Modular values and weak values of quantum observables *Phys. Rev. Lett.* **105** 230401
[61] Cormann M and Caudano Y 2017 Geometric description of modular and weak values in discrete quantum systems using the Majorana representation *J. Phys. A: Math. Theor.* **50** 305302
[62] Ho L B and Imoto N 2018 Various pointer states approaches to polar modular values *J. Math. Phys.* **59** 042107
[63] Samlan C T and Viswanathan N K 2017 Geometric phase topology in weak measurement *J. Opt.* **19** 125401
[64] Pal M, Saha S, Athira B S, Dutta Gupta S and Ghosh N 2019 Experimental probe of weak-value amplification and geometric phase through the complex zeros of the response function *Phys. Rev.* A **99** 032123
[65] Cho Y-W, Kim Y, Choi Y-H, Kim Y-S, Han S-W, Lee S-Y, Moon S and Kim Y-H 2019 Emergence of the geometric phase from quantum measurement back-action *Nat. Phys.* **15** 665–70
[66] Bargmann V 1964 Note on Wigner's theorem on symmetry operations *J. Math. Phys.* **5** 862–8
[67] Gedik Z 2021 Weak measurement of Berry's phase *J. Phys. A: Math. Theor.* **54** 405301
[68] Bengtsson I and Życzkowski K 2017 *Geometry of Quantum States: An Introduction to Quantum Entanglement* (Cambridge: Cambridge University Press)
[69] Kimura G 2003 The Bloch vector for N-level systems *Phys. Lett.* A **314** 339–49
[70] Bertlmann R A and Krammer P 2008 Bloch vectors for qudits *J. Phys. A: Math. Theor.* **41** 235303
[71] Goyal S K, Simon B N, Singh R and Simon S 2016 Geometry of the generalized Bloch sphere for qutrits *J. Phys. A: Math. Theor.* **49** 165203
[72] Siegel C L 2014 *Symplectic Geometry* (Amsterdam: Elsevier)
[73] Hangan T and Masala G 1994 A geometrical interpretation of the shape invariant for geodesic triangles in complex projective spaces *Geom. Dedicata* **49** 129–34

[74] Ortega R and Santander M 2003 Trigonometry of the quantum state space, geometric phases and relative phases *J. Phys. A: Math. Gen.* **36** 459–85
[75] Mukunda N *et al* 2003 Bargmann invariants, null phase curves, and a theory of the geometric phase *Phys. Rev.* A **67** 042114
[76] Macfarlane A J, Sudbery A and Weisz P H 1968 On Gell–Mann's λ-matrices, d- and f-tensors, octets, and parametrizations of SU(3) *Commun. Math. Phys.* **11** 77–90
[77] Arvind , Mallesh K S and Mukunda N 1997 A generalized Pancharatnam geometric phase formula for three-level quantum systems *J. Phys. A: Math. Gen.* **30** 2417–31
[78] Khanna G, Mukhopadhyay S, Simon R and Mukunda N 1997 Geometric phases for SU(3) representations and three level quantum systems *Ann. Phys., NY* **253** 55–82
[79] Byrd M 1998 Differential geometry on SU(3) with applications to three state systems *J. Math. Phys.* **39** 6125–36
[80] Jakóbczyk L and Siennicki M 2001 Geometry of Bloch vectors in two-qubit system *Phys. Lett.* A **286** 383–90
[81] Byrd M S and Khaneja N 2003 Characterization of the positivity of the density matrix in terms of the coherence vector representation *Phys. Rev.* A **68** 062322
[82] Graf A and Piéchon F 2021 Berry curvature and quantum metric in N-band systems: an eigenprojector approach *Phys. Rev.* B **104** 085114
[83] Porto-Silva Y P and de Oliveira M C 2021 Theory of neutrino detection: flavor oscillations and weak values *Eur. Phys. J.* C **81** 330
[84] Cormann M, Remy M, Kolaric B and Caudano Y 2016 Revealing geometric phases in modular and weak values with a quantum eraser *Phys. Rev.* A **93** 042124
[85] Peres A 1991 Two simple proofs of the Kochen–Specker theorem *J. Phys. A: Math. Gen.* **24** L175–8
[86] Maldacena J, Shenker S H and Stanford D 2016 A bound on chaos *J. High Energy Phys.* JHEP08(2016)106
[87] Lundeen J S and Resch K J 2005 Practical measurement of joint weak values and their connection to the annihilation operator *Phys. Lett.* A **334** 337–44
[88] Solli D R, McCormick C F, Chiao R Y, Popescu S and Hickmann J M 2004 Fast light, slow light, and phase singularities: a connection to generalized weak values *Phys. Rev. Lett.* **92** 043601
[89] Hall M 2004 Prior information: how to circumvent the standard joint-measurement uncertainty relation *Phys. Rev.* A **69** 052113
[90] Dressel J 2015 Weak values as interference phenomena *Phys. Rev.* A **91** 032116
[91] Dressel J and Jordan A N 2012 Significance of the imaginary part of the weak value *Phys. Rev.* A **85** 012107
[92] Hofmann H F 2011 Uncertainty limits for quantum metrology obtained from the statistics of weak measurements *Phys. Rev.* A **83** 022106
[93] Hofmann H F 2021 Direct evaluation of measurement uncertainties by feedback compensation of decoherence *Phys. Rev. Res.* **3** L012011
[94] Pusey M F 2014 Anomalous weak values are proofs of contextuality *Phys. Rev. Lett.* **113** 200401
[95] Kunjwal R, Lostaglio M and Pusey M F 2019 Anomalous weak values and contextuality: robustness, tightness, and imaginary parts *Phys. Rev.* A **100** 042116